Matter

CellPress

Review

Black phosphorus-based nanomedicines

Yijie Fan,[1,2,3,6] Liyuan Chen,[2,6] Jingning Zhang,[1,3,6] Cong Liu,[1,3,*] Linsu Liu,[1,3] Ruizeng Luo,[1,3] Shiwang Xie,[1,3] Zhou Li,[4,5,*] Yan Liu,[2,*] and Dan Luo[1,3,*]

[1]Beijing Institute of Nanoenergy and Nanosystems, Beijing Key Laboratory of High-Entropy Energy Materials and Devices, Chinese Academy of Sciences, Beijing 101400, P.R. China

[2]Central Laboratory, Department of Orthodontics, Peking University School and Hospital for Stomatology & National Center for Stomatology & National Clinical Research Center for Oral Diseases & National Engineering Research Center of Oral Biomaterials and Digital Medical Devices & Beijing Key Laboratory of Digital Stomatology & Research Center of Engineering and Technology for Computerized Dentistry Ministry of Health & NMPA Key Laboratory for Dental Materials & National Engineering Research Center of Oral Biomaterials and Digital Medical Devices, Beijing 100081, P.R. China

[3]School of Nanoscience and Engineering, University of Chinese Academy of Sciences, Beijing 100049, P.R. China

[4]Beijing Tsinghua Changgung Hospital, School of Clinical Medicine, Tsinghua University, Beijing 100084, P.R. China

[5]School of Biomedical Engineering, Tsinghua University, Beijing 100084, P.R. China

[6]These authors contributed equally

*Correspondence: liucong@binn.cas.cn (C.L.), li_zhou@tsinghua.edu.cn (Z.L.), orthoyan@bjmu.edu.cn (Y.L.), luodan@binn.cas.cn (D.L.)

https://doi.org/10.1016/j.matt.2025.102634

PROGRESS AND POTENTIAL Nanomedicine is reshaping therapeutic paradigms by emphasizing precision, controllability, and multifunctionality, with nanomaterials increasingly transitioning from passive carriers to active therapeutic agents. Black phosphorus (BP), an emerging two-dimensional nanomaterial, has attracted considerable attention owing to its distinctive physicochemical properties and intrinsic biodegradability. These features enable efficient transduction of external physical stimuli into heat and reactive oxygen species, supporting its application in multimodal treatment strategies. Beyond stimulus-driven effects, accumulating evidence indicates that BP-based nanomedicines (BP NMs) can directly and dynamically interact with biological systems, thereby actively modulating biological processes.

At the same time, BP NM-biological interactions are highly contingent on cellular and microenvironmental contexts, representing both an opportunity and a source of ongoing debate. Current studies often consider therapeutic efficacy and biosafety in isolation, with limited integration of material properties and biological responses. Systematically mapping the structure-property-bioresponse relationships of BP NMs is therefore essential for establishing a unified mechanistic framework. Such insights will guide the rational and safe design of BP NMs and enhance their translational potential.

SUMMARY

Nanomedicines (NMs) have demonstrated considerable promise in the treatment of diverse diseases. Their dynamic interactions with biological systems often trigger a cascade of complex physiological responses. Revealing the structure-activity relationships that underlie these interactions is critical for the rational design of safer and more effective nanotherapeutics. Among emerging two-dimensional (2D) nanomaterials, black phosphorus (BP) has garnered increasing interest owing to its unique physicochemical properties and inherent biodegradability. Featuring a tunable bandgap, high carrier mobility, and excellent biocompatibility, BP exhibits significant potential in biomedical applications. Due to its multidimensional functional characteristics, BP can elicit a variety of distinct biological effects upon interfacing with biological systems, including oxidative stress, ionic disturbance, and immune activation. A comprehensive understanding of these regulatory effects and their underlying mechanisms will help promote the broader medical application and even clinical translation of BP-based NMs (BP NMs). In this review, we systematically summarize the application of BP as NMs in cancer treatment, tissue engineering, and regenerative medicine based on its intrinsic biological effects rather than carrier effects, and further elaborate the mechanisms underlying BP's interactions with biological systems across these contexts. Comprehensively mapping the relationship between the structure, properties, and biological activity of BP will provide directions for the future design aimed at improving the safety and effectiveness of BP NMs.

INTRODUCTION

Nanomedicine (NM) is fundamentally reshaping conventional therapeutic paradigms with the core principles of precision, controllability, and integration. These principles have spurred the emergence of diverse innovative treatment modalities, including photothermal therapy (PTT), photodynamic therapy (PDT), and sonodynamic therapy (SDT), as well as a spectrum of combined approaches. In these emerging therapies, nanomaterials function not merely as drug delivery vehicles but also as therapeutic agents whose inherent physicochemical properties can amplify and synergize with loaded cargos. Furthermore, the biological responses elicited by nanomaterials *in vivo* are remarkably complex and intricately dependent on their structural and chemical attributes. A comprehensive understanding of the structure-function relationship and toxicological profile of nanomaterials is therefore essential for their safe and effective translation into clinical practice.

Black phosphorus (BP), a novel two-dimensional (2D) nanomaterial,[1] has garnered widespread attention due to its tunable bandgap, negative Poisson's ratio,[2] in-plane anisotropy,[3] and biocompatibility.[4] These characteristics endow BP with wide-ranging potential in applications spanning energy catalysis, optoelectronics, biosensing, and biomedicine. Owing to its distinctive electronic structure and broadband light absorption capability, BP can efficiently respond to external physical stimuli and convert them into endogenous thermal energy and reactive oxygen species (ROS), thereby demonstrating exceptional therapeutic efficacy in cancer treatment and antimicrobial applications. Moreover, the high reactivity of phosphorus atoms and the biocompatible degradation products of BP open up new avenues in biomedical applications, particularly in modulating oxidative stress and cellular energy metabolism (EM).

Recently, accumulating evidence has uncovered the distinctive biological behaviors induced by BP *in vivo*. Despite considerable advances, formidable challenges persist in translating fundamental discoveries into clinical practice, and certain biological effects associated with BP-based NMs (BP NMs) remain controversial. Initial investigations reported favorable biocompatibility, attributing it to BP's degradability into non-toxic phosphate species. However, subsequent findings have revealed that the biosafety of BP is influenced by multiple parameters, including particle concentration, size, and surface functionalization. Notably, by liberating essential phosphate ions (PO_4^{3-}), BP's biodegradability functions as a double-edged sword,[5] simultaneously supporting biological activity and potentially perturbing cellular homeostasis through ionic interference. Moreover, upon entry into biological systems, BP inevitably interacts with cells, subcellular organelles, and biomacromolecules. These interactions, coupled with its elemental composition and biochemical reactivity, can provoke unpredictable biological responses.[6,7] Thus, a systematic and in-depth exploration of BP's physicochemical properties and their consequent *in vivo* bioeffects is in urgent demand. To date, most studies have focused either on the therapeutic efficacy or the biocompatibility of BP nanomaterials in isolation, with limited emphasis on the intrinsic connections between their material properties and biological activity. Therefore, a comprehensive review of BP's material characteristics and their corresponding biological responses is crucial for the rational design of safer and more efficacious BP NMs.

In this review, we categorize the biological activities of BP NMs into three principal mechanisms: (1) bioactivity driven by physical stimuli; (2) physiological modulation mediated by chemical reactivity, particularly redox interactions; and (3) direct biointeractions with biomolecules, organelles, and cells (Figure 1). First, we introduce the structure and physiochemical characteristics of BP. Then, we summarize its representative bioactivities in biomedical applications and their potential mechanisms, such as heat stress, oxidative stress, and immune activation. Finally, we discuss the potential applications and challenges of BP in medicine.

STRUCTURAL BASIS AND MULTIDIMENSIONAL PERFORMANCE CHARACTERISTICS OF BP

As a 2D material that uniquely integrates structural tunability with chemical plasticity, BP offers an ideal model system for elucidating how atomic-scale architectures govern multidimensional properties. Its anisotropic structure yields strongly coupled responses to optical, electrical, and mechanical stimuli, while tunable bandgaps across thicknesses broaden its operational window for photoelectric conversion and energy transduction. The surface-exposed lone-pair electrons confer exceptional chemical reactivity, enabling redox catalysis, metal ion coordination, and radical modulation, yet simultaneously render BP vulnerable to rapid degradation in physiological environments. This intrinsic ''high activity-low stability'' dichotomy positions BP at the forefront of catalysis, bioimaging, and microenvironment engineering, and underscores the need for precise stability control. Rapid advances in surface and interface engineering, including covalent modification, metal ion coordination, and polymer or biofilm encapsulation, have markedly improved BP stability, attenuated excessive surface reactivity, and generated heterointerfaces with emergent electronic characteristics, thereby reshaping its photocatalytic and biological performance. Within living systems, BP's dynamic interactions with proteins and lipids govern its biotransformation pathways and exert profound effects on cellular redox homeostasis and stress signaling.

Structure, intrinsic semiconductor properties, and associated physical effects of BP

Atomic structure of BP

In 1914, Bridgman et al.[8] synthesized bulk BP crystals under high-pressure conditions of 1.2 GPa and a temperature of 200°C. However, there was little interest in this black crystal at the time. Then, in 2014, multiple research groups revisited BP's properties from the vantage point of nanoscale flakes. This reevaluation yielded unprecedented achievements, reigniting interest in BP after nearly a century.[9] BP is a multilayered crystal featuring a graphene-like structure, in which individual layers are held together by van der Waals forces. The interlayer spacing varies between 3.21 Å and 3.73 Å. Monolayer BP consists of sp^3 hybridized phosphorus atoms, each bonded to three neighboring atoms via covalent bonds and bearing a lone pair of

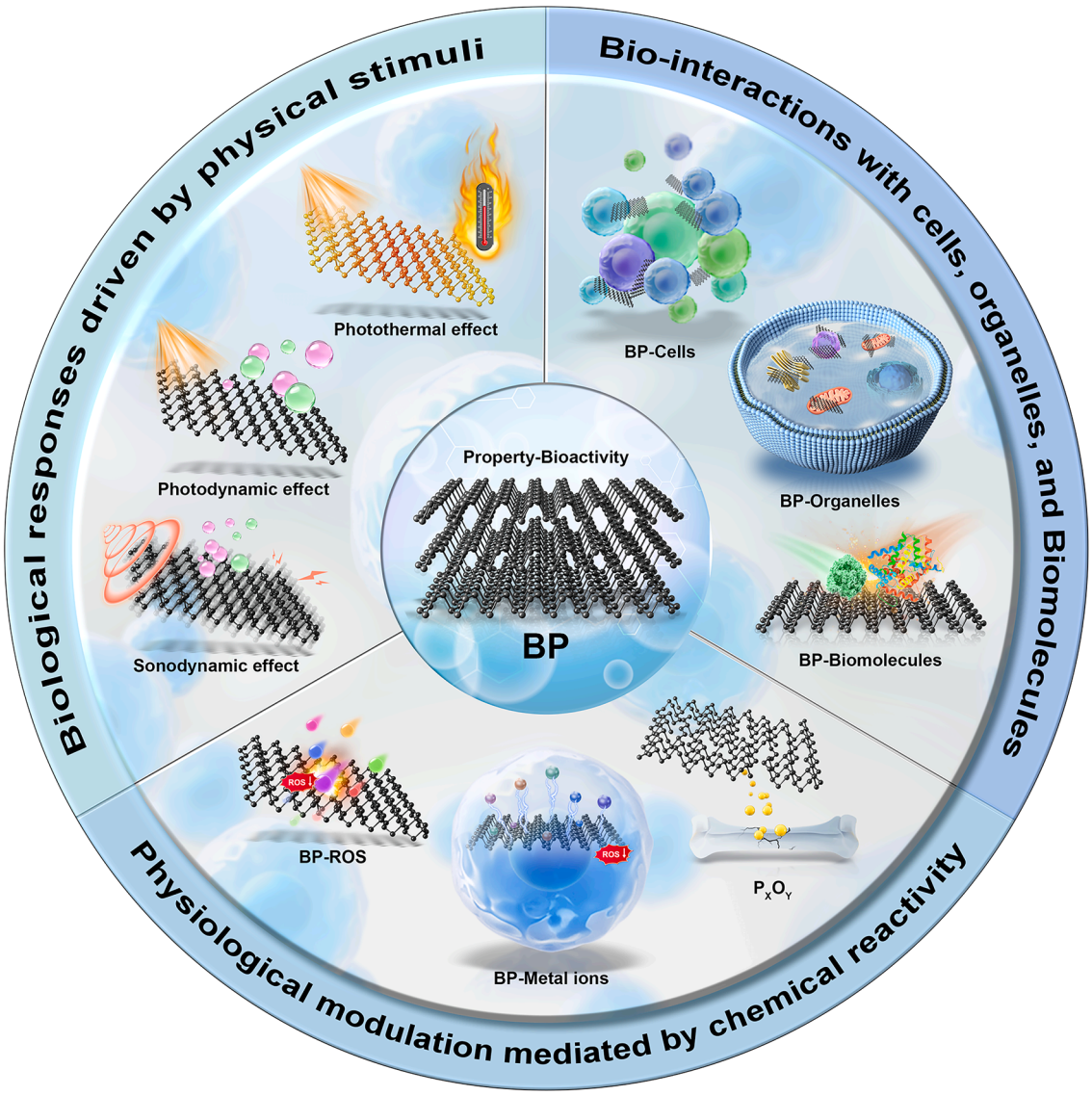

Figure 1. Physical-chemical characteristics and representative bioactivities of BP

Schematic overview of three principal mechanisms underlying BP bioactivity: physical stimulus-driven effects, chemical reactivity-mediated physiological modulation, and direct interactions with biomolecules, organelles, and cells.

electrons.[10,11] This unique combination bestows monolayer BP with a structure similar to a folded honeycomb. Notably, monolayer BP presents divergent structures when viewed from distinct directions-armchair in the Z direction and zigzag in the X direction.[12] This significant in-plane anisotropy of BP emerges from its distinctive structural arrangement (Figure 2A). The interlayer interaction in BP arises from van der Waals forces between non-bonding lone electron pairs.[13] Consequently, applying external force enables exfoliation into few-layer or monolayer BP nanomaterials. The optoelectronic properties of BP are layer-dependent and tunable,[14] providing a theoretical foundation for designing versatile NMs adaptable to diverse applications.

Semiconductor properties and physical stimulus response performance of BP

By modulating layer thickness and applying strain,[20,21] the band gap of BP can be tuned across a broad range from 0.3 to 2.0 eV.[22] This tunability enables BP to absorb light spanning the ultraviolet (UV) to infrared spectrum. Such broad spectral absorption underscores the significant potential of BP NMs for applications in optical imaging and therapeutic interventions.[16,23] Sun et al.[16] demonstrated that BP quantum dots (BPQDs) possess a broad absorption spectrum spanning the UV to near-infrared (UV-NIR) range, with an outstanding extinction coefficient of 14.8 $L \cdot g^{-1} \cdot cm^{-1}$ at 808 nm (Figure 2B). Upon 10 min of 808 nm laser irradiation, a 50 ppm aqueous solution of BPQDs

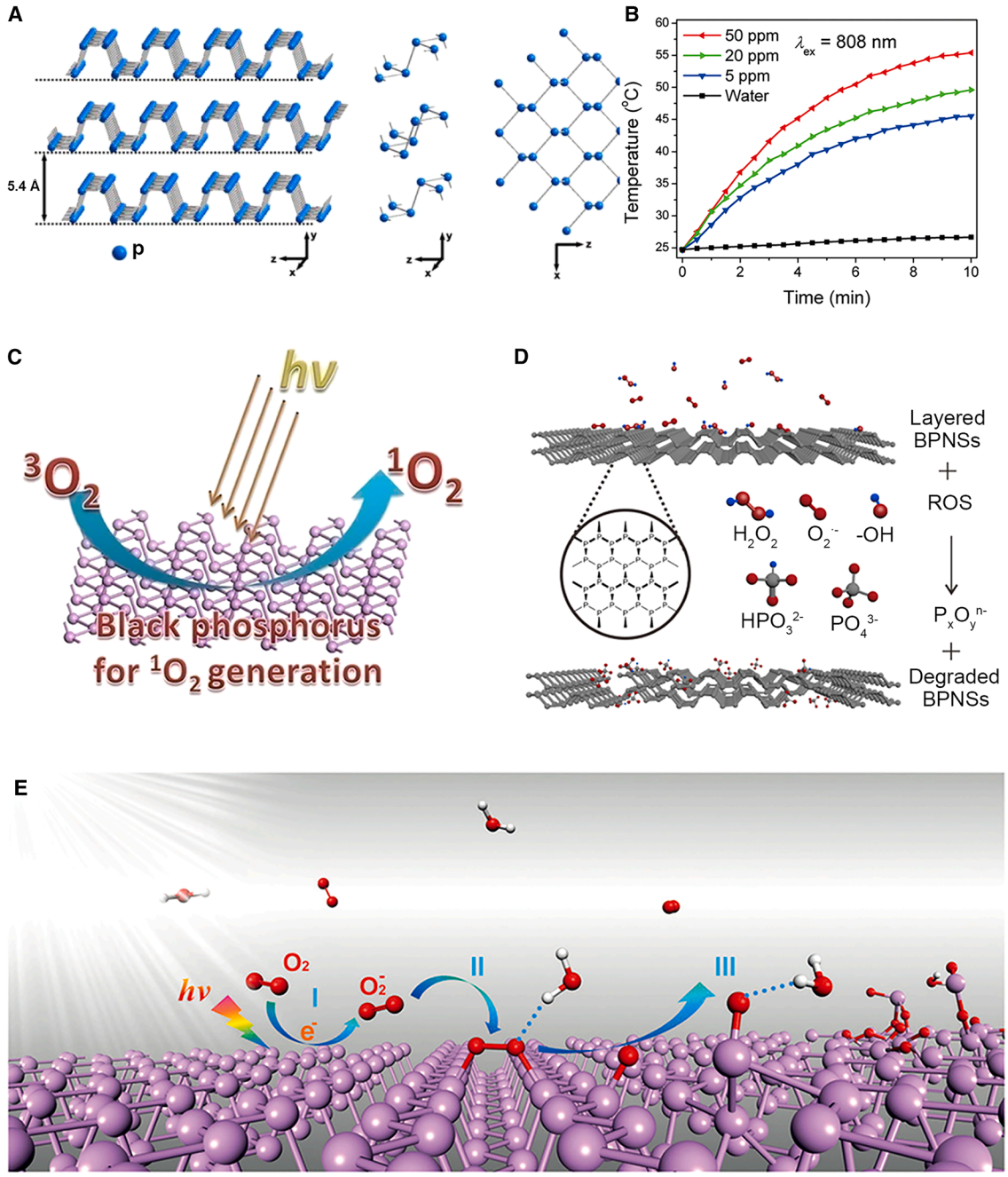

Figure 2. Structure and physicochemical properties of BP

(A) Structure of BP crystal.[15] Copyright 2017, American Chemical Society.

(B) Photothermal heating curves of BPQDs dispersed in water under irradiation with an 808 nm laser.[16] Copyright 2015, Wiley-VCH.

(C) BP NSs generate ROS under light irradiation.[17] Copyright 2015, American Chemical Society.

(D) The reaction between BP NSs and ROS.[18] Copyright 2020, American Chemical Society.

(E) Light-induced degradation of BP in the environment.[19] Copyright 2016, Wiley-VCH.

exhibited a temperature increase of 31.5°C, corresponding to a remarkable photothermal conversion efficiency of 28.4%, surpassing that of commercial Au nanoshells.[24,25] In addition, the intrinsic semiconductor properties of BP nanomaterials allow them to harness external energy, such as light, ultrasound (US), or mechanical force, to generate electron-hole pairs. These excited carriers subsequently engage in redox reactions, leading to the production of ROS or the modulation of physiological processes. Wang et al.[17] prepared BP nanosheets (BP NSs) via ultrasonic liquid-phase exfoliation; under 660 nm laser exposure,

these NSs markedly enhanced singlet oxygen ($^1O_2$) generation compared to bulk BP (Figure 2C). This enhancement stemmed from their ultrathin morphology, which effectively suppressed electron-hole recombination. Collectively, the unique structural and optoelectronic properties of BP nanomaterials position them as promising candidates for tumor phototherapy and drug delivery.

Chemical reactivity of BP

Electronic structure and chemical reactivity of BP

In BP, phosphorus atoms adopt sp^3 hybridization, forming covalent bonds with three neighboring atoms while retaining a lone pair of electrons. This distinctive structural configuration endows it with exceptional chemical reactivity and underlies its unique chemical behavior. The lone pairs on the surface phosphorus atoms exhibit pronounced reactivity toward water, O_2, and ROS, imparting a Janus-faced role in biological applications: they confer exceptional biocompatibility and antioxidant capacity (Figure 2D), yet simultaneously render the crystal lattice vulnerable to structural damage, which may impair its physical properties. Furthermore, phosphorus atoms with high surface energy can also coordinate with metal ions through orbital hybridization and serve as *in situ* reduction sites for metal ions. These remarkable chemical attributes form the foundation for the broad utility of BP in biomedicine and biocatalysis. Favron et al.[26] reported that the oxidation of BP NSs initiates at the surface. Upon exposure to ambient air for several days, the crystalline structure of BP was almost entirely disrupted due to the synergistic effects of oxygen and moisture, and its overall morphology changed to a droplet shape. Zhou et al.[19] proposed a more comprehensive degradation mechanism. Under illumination, photogenerated charge carriers are produced on the BP surface and subsequently react with adsorbed oxygen molecules to form superoxide anions. These reactive species further interact with non-bonded lone-pair electrons on the BP surface, leading to the formation of phosphorus oxides (Figure 2E). Water molecules then remove the resulting P_xO_y species via hydrogen bonding, exposing internal phosphorus atoms and thereby perpetuating the oxidation cascade.[27] This property indicates that BP can elicit distinctive therapeutic outcomes, particularly in scavenging ROS and alleviating oxidative stress-related diseases.[18] Paradoxically, the same highly reactive lone pairs that endow BP with therapeutic potential—through rapid degradation into non-toxic PO_4^{3-} and alleviation of oxidative stress—also render it susceptible to structural disruption and loss of photoelectric performance. Thus, balancing "reactivity" and "stability" is essential to preserve both biosafety and functional integrity. A mechanistic understanding of BP degradation is therefore critical to enable its controlled and efficacious application.

Surface modification strategies for BP NMs

The atomic structure and electronic properties of BP underpin its distinctive physicochemical characteristics. Reinforcing its stability under physiological conditions is therefore essential to preserving its intrinsic properties and realizing optimal therapeutic outcomes. Owing to its open surface architecture and highly reactive phosphorus atoms, the photoelectric properties of BP can be tuned via surface modifications. Current strategies primarily focus on mitigating or shielding the interaction between surface-exposed lone pair electrons and oxygen molecules, typically through surface passivation or the incorporation of protective coatings, to enhance environmental stability and biocompatibility. Ryder et al.[28] promoted the environmental stability of BP by covalently attaching aryldiazonium molecules, forming stable P-C bonds that effectively passivated the surface-active lone pair electrons.[29] This strategic modification not only significantly improved the chemical robustness of BP but also enhanced its electronic properties (Figure 3A). Additionally, metal ions have been shown to inhibit oxidative degradation by coordinating with the surface lone pairs of BP. Guo et al.[30] further demonstrated that free metal ions (e.g., Ag^+, Fe^{3+}, Mg^{2+}, and Hg^{2+}) could interact with BP through cation-π interactions, effectively stabilizing the material against oxidation (Figure 3B). This unique reactivity enables BP to engage selectively with various bioactive molecules, thereby endowing it with unanticipated therapeutic functionalities.

The incorporation of polymers or biofilms with BP represents a prevalent passivation strategy. Polymer/BP and biofilm/BP composites are garnering considerable attention in biomedicine due to their non-toxic nature and mild synthesis conditions. Tao et al.[31] successfully introduced surface modification to BP NSs using polyethylene glycol amine (PEG-NH_2), primarily via electrostatic interactions (Figure 3C). The PEG-NH_2 modification imparted outstanding dispersibility and stability in physiological media, while concurrently enhancing photothermal performance. Shao et al.[32] employed the emulsion method to fabricate poly(lactic-co-glycolic acid) (PLGA)-encapsulated BPQD nanospheres (Figure 3D). A comprehensive series of *in vivo* and *in vitro* experiments unequivocally revealed good biocompatibility and remarkable photothermal properties of these prepared nanospheres, which facilitated the efficient ablation of deep-seated tumors. In addition, Liu et al.[33] harnessed electroporation to encapsulate BPQDs within exosomes (EXOs). Experimental findings affirmed that these nanospheres exhibited superior stability and photothermal properties compared to bare BPQDs.

Biocompatibility and toxicological evaluation of BP

The biological toxicity of nanomaterials is closely linked to their physicochemical properties. BP nanomaterials are generally regarded as biocompatible, owing to their ultimate degradation into non-cytotoxic phosphorus oxides. However, accumulating evidence suggests that the cytotoxicity of BP remains contentious. Rather than being an intrinsic property, the toxicity of BP nanomaterials is a dynamic characteristic influenced by multiple parameters, including particle size, morphology, surface chemistry, and biotransformation *in vivo*. Accordingly, precise modulation of these physicochemical features is essential to ensure their safe use in biomedical applications. Lee et al.[34] demonstrated that both BP nanodots and their degradation products (PO_4^{3-}) exhibited minimal cytotoxicity *in vitro*. Song et al.[35] showed that BP NSs display time- and dose-dependent cytotoxicity, with a markedly stronger killing effect on fibrosarcoma (HT1080) than on normal fibroblasts (nHDF and NIH3T3), following the order HT1080 > nHDF > NIH3T3. Chen et al.[36] observed that both BP NSs and PEG-BP NSs at concentrations

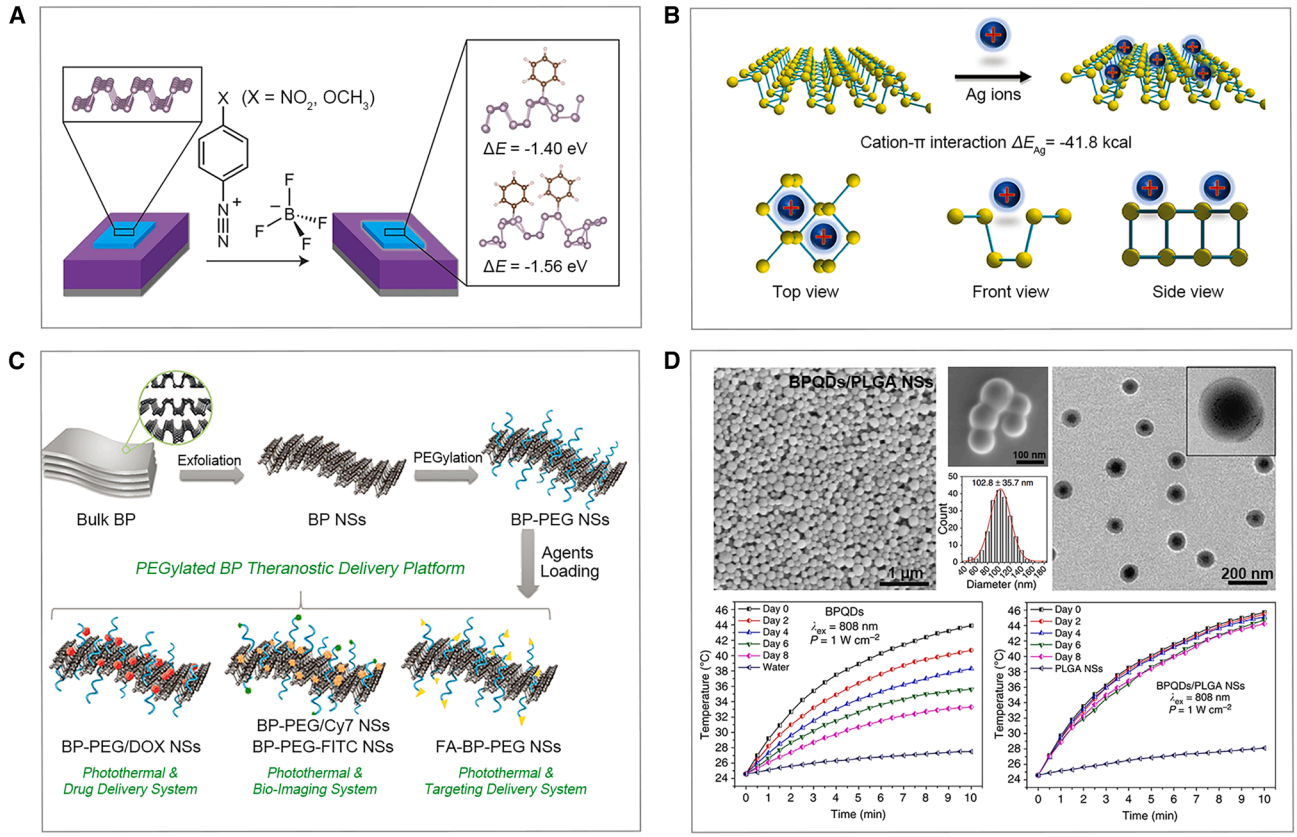

Figure 3. Surface modification strategies of BP NMs

(A) Covalent grafting of benzene-diazonium tetrafluoroborate derivatives for enhanced BP environmental stability.[28] Copyright 2016, Springer Nature.

(B) Reaction between BP and Ag^{+}.[30] Copyright 2017, Wiley-VCH.

(C) Synthesis of the pegylated BP nanodelivery platform.[31] Copyright 2016, Wiley-VCH.

(D) Structure and photothermal temperature rise curves of BPQDs/PLGA.[32] Copyright 2016, Springer Nature.

of 0.8 μg mL^{-1} elicited marked cytotoxicity in human umbilical vein endothelial cells (HUVECs), accompanied by pronounced morphological alterations. Moreover, at a lower concentration (0.4 μg mL^{-1}), both materials compromised endothelial barrier integrity by downregulating the expression of the tight junction-associated protein zona occludens-1 (ZO-1). Complementarily, Zhang et al.[37] systematically assessed BP's biological toxicity and highlighted its dependence on particle size, concentration, and cell type. The studies confirmed that PO_4^{3-} produced during BP degradation exerted a negligible impact on cellular viability. *In vitro* experiments further revealed that reducing the lateral size, thickness, and concentration of BP NSs significantly attenuated their cytotoxicity. Notably, cell membrane disruption and elevated intracellular ROS levels were identified as key contributors to size-dependent cytotoxic effects.

In addition to the well-established size- and concentration-dependent toxicity,[38] BP NMs may engage in complex interactions with bioactive molecules—such as proteins, enzymes, and lipids—within the cellular microenvironment upon entering the body. These interactions can markedly alter the surface chemistry, biodistribution, and cellular uptake pathways of BP NMs, thereby modulating cellular behavior and potentially triggering toxic responses.[39] For instance, the non-bonded lone pair electrons on the BP surface readily bind to biomacromolecules, potentially disrupting critical physiological processes, including cell cycle progression, mitochondrial function, mitotic centrosome destabilization, and ROS homeostasis. Furthermore, intracellular degradation of BP NMs may disturb anion homeostasis, thereby impacting cellular signaling and metabolic functions. Toxicological studies have also demonstrated that BP NMs possess proinflammatory and immunostimulatory capabilities. Specifically, BP NSs have been shown to elevate intracellular ROS levels and promote the release of proinflammatory cytokines in macrophages via activation of the nuclear factor kappa B (NF-κB) signaling pathway, while concurrently suppressing the expression of the anti-inflammatory mediator heme oxygenase-1 (HO-1),[40] thereby exacerbating inflammatory responses. Wang et al.[41] further reported that BP NMs could induce systemic inflammation by disrupting the generation and migration of immune cells. Therefore, comprehensively elucidating the interaction mechanisms between BP NMs and bioactive molecules is of critical significance for a thorough assessment of their biosafety and successful translation into clinical practice.

BIOACTIVITY DERIVED FROM PHYSICOCHEMICAL PROPERTIES OF BP

As an emerging 2D semiconductor, BP has attracted widespread attention due to its distinctive physicochemical properties. Its unique electronic structure makes it highly sensitive to external physical stimuli, such as light and US, thereby enabling diverse and robust functional responses suited for a broad range of biomedical diagnostic and therapeutic applications. Moreover, BP possesses an open surface structure that fully exposes all phosphorus atoms to the surrounding environment. The lone electron pairs and dangling bonds on these atoms contribute to its high chemical reactivity, allowing BP to act both as a generator of ROS and as a potential antioxidant in biological settings. Additionally, the phosphorus oxides formed during the degradation of BP *in vivo* serve as bioavailable phosphate sources. These not only support bone mineralization and EM but also exert regulatory effects on various cellular signaling pathways. Notably, the active surface of BP can directly interact with cells and bioactive molecules, thereby influencing critical biological processes such as oxidative stress, immune activation, programmed cell death, and metabolic homeostasis.

Bioactivity based on physical stimulus responsiveness of BP

Owing to its unique layered architecture and multidimensional physicochemical properties—including a tunable bandgap, high carrier mobility, strong photoresponsiveness, and intrinsic piezoelectric effect—BP can elicit multifaceted and sophisticated biological responses *in vivo*. Leveraging these attributes, BP NMs have demonstrated remarkable therapeutic potential across a wide spectrum of biomedical applications, such as PTT, PDT, and SDT.

Bioregulation based on the photothermal effect of BP

As a compelling modality for tumor treatment, PTT harnesses the thermal effect generated by photothermal agents at the target site to ablate cancerous tissue.[42] In comparison to conventional treatment modalities, PTT offers simplicity, minimal invasiveness, fewer side effects, and shorter treatment durations.[43] This novel therapeutic paradigm has already yielded tremendous success in clinical trials and holds the potential for a revolutionary impact on clinical practice. Among the numerous nanophotothermal agents, BP NMs have garnered considerable attention due to their exceptional biocompatibility, biodegradability, and high photothermal conversion efficiency. Sun et al.[16] successfully synthesized BPQDs via a synergistic approach combining probe and ice-bath ultrasonication, demonstrating their exceptional photothermal conversion efficiency and stability. Upon NIR irradiation, the generated heat effectively ablated C6 and MCF-7 cells. Tao et al.[44] integrated ultrathin BP NSs into an injectable fibrin gel, yielding a smart BP-based gel with rapid *in situ* gelation, pronounced NIR responsiveness, and robust photothermal conversion. Upon NIR irradiation, the system undergoes swift localized heating, enabling on-demand acceleration of drug release while simultaneously exerting potent antibacterial activity and facilitating tissue regeneration. Furthermore, Wang et al.[45] engineered a minimally invasive therapeutic intravenous catheter incorporating BP NSs for *in vivo* capture and elimination of circulating tumor cells (CTCs). Functionalization of the catheter surface with anti-epithelial cell adhesion molecule (EpCAM) antibodies enabled efficient CTC recognition and binding, while the outstanding photothermal properties of BP NSs facilitated the complete ablation of captured CTCs under NIR light.

During PTT, cancer cells can initiate heat shock and other stress-response pathways, markedly attenuating treatment efficacy.[46] Suppressing these protective mechanisms has emerged as a promising strategy to enhance PTT sensitivity. Chen et al.[47] employed supercritical fluid (SCF) technology to encapsulate both BPQDs and gambogic acid (GA) within poly(L-lactide)-poly(ethylene glycol)-poly(L-lactide) triblock copolymer (PLLA-PEG-PLLA), yielding BPQDs/GA/PLLA-PEG-PLLA (BGP) nanocomposites. These nanocomposites were designed for photoacoustic (PA) imaging-guided chemotherapy-photothermal synergistic therapy. BGP could generate local hyperthermia at the tumor site while promoting the release of GA. GA, in turn, mitigated the resistance of tumor cells to high temperatures by selectively binding to heat shock protein (HSP)-90 produced during cellular heat stress, thus causing tumor cells to succumb to BPQD-induced PTT (Figure 4A). Moreover, Xie et al.[48] discovered that PTT induced by BP NSs could stimulate cells to produce stress granules (SGs), fostering heat resistance within tumors and diminishing the sensitivity of tumor cells to PTT. To counteract this effect, they developed a hydrogel platform incorporating BP NSs and the SG inhibitor emetine. Upon NIR irradiation, BP NSs generated hyperthermia capable of eradicating tumor cells. Simultaneously, the controlled release of emetine in response to light suppressed SG formation within tumor cells, heightening their sensitivity to PTT and consequently enhancing the therapeutic effects of PTT.

Furthermore, BP's inherent instability under physiological conditions, which renders it susceptible to degradation, can impair its photoelectric properties and consequently limit its efficacy in tumor phototherapy. The application of surface passivation strategies has been shown to preserve its photothermal performance and enhance stability in biological environments. Zhao et al.[50] found that titanium sulfonate ligand (TiL_4)-modified BP NSs (TiL_4@BP) exhibited strengthened photothermal stability compared to the bare BP NSs and demonstrated a more pronounced effect on *in vitro* cancer cell eradication. Meanwhile, Sun et al.[25] produced PEG-modified BP nanoparticles (NPs) via a simple one-pot method, optimizing the NPs' water solubility and biocompatibility.[51] Leveraging the enhanced permeability and retention (EPR) effect of tumors, these NPs could effectively accumulate at tumor sites, enabling PA imaging-guided PTT. Furthermore, Deng et al.[52] used engineered dextran- and polyethylenediimine-functionalized BP NPs, further modifying them with folate (FA) and Cy7. This modification endowed BP NPs (BP-DEX/PEI-FA/Cy7) with active targeting capabilities and NIR fluorescence (NIRF) imaging functionalities. *In vivo* experiments validated the good biocompatibility, high photothermal conversion efficiency, and exceptional tumor clearance efficiency of BP-DEX/PEI-FA/Cy7. Deng et al.[49] also harnessed superparamagnetic iron selenide ($FeSe_2$) to covalently modify BP NSs, creating NPs (BPs-$FeSe_2$-PEG) with good water solubility. These Se atom modifications on the surface of BP NSs

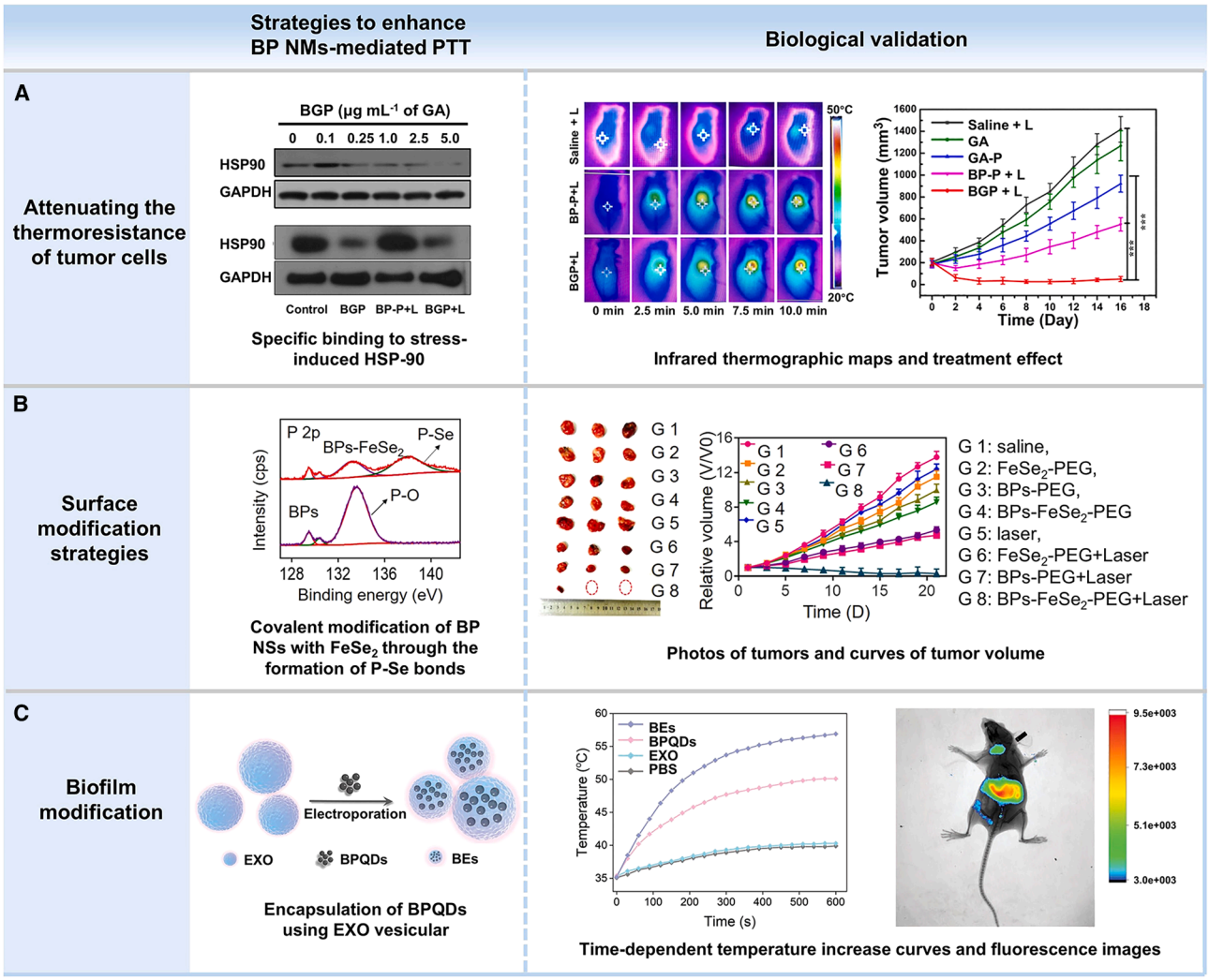

Figure 4. Strategies for enhancing BP NMs-mediated PTT

(A) BGP sensitizes tumor cells to PTT through HSP-90 binding (n = 6).[47] Data are expressed as the mean ± standard deviation (SD). Copyright 2020, Elsevier.

(B) Covalent $FeSe_2$ modification of BP NSs enhances their stability and PTT efficacy (n = 3).[49] Data are expressed as the mean ± SD. Copyright 2021, Springer Nature.

(C) Exosome encapsulation enhances blood circulation stability and photothermal efficacy of BPQDs.[33] Copyright 2021, Wiley-VCH.

occupied the lone pairs of electrons, augmenting the stability of BP NSs. Additionally, the BPs-$FeSe_2$-PEG heterostructure facilitated the separation of photogenerated carriers, further enhancing BP's photothermal conversion efficiency. *In vivo* experiments demonstrated the potential of magnetic resonance imaging (MRI)-guided PTT for precise tumor elimination (Figure 4B).

Due to their ultrasmall size, BPQDs are highly prone to oxidation by water and oxygen under physiological conditions, which markedly compromises their efficacy in PTT. To overcome this limitation, surface modification strategies have been developed to effectively shield BPQDs from oxidative degradation, prolong their blood circulation time, and enhance tumor-specific accumulation, ultimately improving the therapeutic effects of PTT. Li et al.[53] devised polydopamine (PDA)-encapsulated BPQDs (BP@PDA), wherein the external PDA layer serves to insulate the BPQDs from direct contact with oxygen and water. Furthermore, PDA, enriched in phenolic groups, can act as a scavenger of ROS, further mitigating BPQD oxidation. This synergy between PDA and BPQDs bolstered the photothermal performance of BP@PDA in aqueous environments. Meanwhile, Shao et al.[54] employed the emulsion method to create PLGA-encapsulated BPQD nanospheres. The PLGA encapsulation effectively preserved the exceptional photothermal properties of BPQDs. Upon NIR irradiation, BPQDs induced deep-tissue photothermal effects, prompting cancer cell apoptosis and the efficient removal of deep-seated tumors.[32] Recent years have witnessed the extensive use of biological carriers, such as cell membranes and extracellular vesicles (EVs), for drug and NP delivery, owing to their low immunogenicity, biocompatibility, and unique natural properties. Liu et al.[33]

employed electroporation to encapsulate BPQDs within EXOs, constructing BPQDs@EXO nanospheres (BEs). The strong biocompatibility and immune evasion capabilities of EXOs enhanced the circulation time of BEs in the bloodstream.[55] The EXO membrane concurrently mitigated the impact of oxygen and water on BPQDs, enhancing BPQDs' stability and consequently augmenting the photothermal treatment efficacy of BEs (Figure 4C). Furthermore, Zhao et al.[56] engineered a biomimetic nanoplatform comprising cancer cell membrane-encapsulated BPQDs. The cell membrane encapsulation significantly improved BPQDs' photothermal stability. Under NIR irradiation, BPQD-mediated PTT could directly eliminate tumor cells and induce dendritic cell (DC) maturation, leading to enhanced antitumor activity. This novel approach effectively curbed the recurrence and metastasis of triple-negative breast cancer (TNBC). Additionally, Luo et al.[57] harnessed the specific targeting ability and low immunogenicity of mesenchymal stem cells (MSCs) toward U251 cells. They encapsulated PLGA/BPQDs into MSCs and used their targeting capability to transfer PLGA/BPQDs into U251 cells. By leveraging the photothermal properties of PLGA/BPQDs, they effectively eradicated U251 cells.

Bioregulation based on the photodynamic effect of BP

PDT operates via light-induced activation of photosensitizers, facilitating energy transfer to nearby oxygen molecules and producing high levels of ROS.[58,59] During BP-mediated PDT, the generated ROS exhibit strong reactivity toward essential cellular components, including membrane lipids, proteins, and DNA, causing oxidative damage that compromises membrane integrity, disrupts protein function, and induces DNA damage, ultimately leading to cell apoptosis. Notably, the diffusion range of ROS in biological systems is limited to approximately 0.1 μm, conferring a highly localized cytotoxic effect. This spatial precision allows PDT to selectively ablate pathological tissues while minimizing collateral damage to surrounding healthy structures, offering a distinct advantage over conventional therapies.[60] Wang et al.[17] demonstrated that BP NSs could act as effective photosensitizers to generate $^1O_2$. Theoretical calculations revealed a quantum yield as high as 0.91 for BP NSs, surpassing that of most commercial photosensitizers. Guo et al.[61] further showed that BPQDs exhibited remarkable efficacy as photosensitizers for tumor treatment. Owing to their ultrasmall size, BPQDs facilitated deep tissue penetration and enhanced PDT outcomes. Additionally, they could be efficiently cleared through autologous renal excretion following intravenous administration, ensuring minimal systemic toxicity.

Harnessing the photodynamic properties of BP offers a promising strategy for antibacterial therapy. Upon light activation, BP functions as an efficient photosensitizer, generating ROS that oxidatively disrupt bacterial membranes or proteins, thereby achieving potent bactericidal effects. Moreover, the readily functionalizable surface of BP enables its integration with complementary antibacterial modalities, such as metal ions, to further enhance therapeutic efficacy. Liang et al.[62] prepared a BP-based Ag antibacterial agent (BPN-Ag NPs) by *in situ* reduction of Ag NPs on BP NSs. The integration of Ag NPs not only bolstered the stability of BP NSs but also amplified the adsorption and activation of O_2, resulting in a remarkable augmentation of ROS generation. The petite size of Ag NPs, measuring less than 10 nm, heightened the affinity of BPN-Ag NPs for bacteria, culminating in a powerful synergistic antibacterial effect (Figure 5A). Furthermore, compared to silver-based alternatives, copper-based antibacterial agents have garnered significant attention due to their low price and excellent antibacterial activity.[63] Zhang et al.[64] developed a BP antibacterial platform loaded with copper NPs using a hydrothermal redox method. The interfacial charge transfer between Cu and BP enhanced the ROS generation efficiency of BP NSs, consequently strengthening the antibacterial activity of the nanoplatforms. Owing to their efficient generation of ROS and inherent bioactivity, BP NMs not only demonstrate potent antibacterial efficacy but also exhibit remarkable advantages in synergistic therapy, such as the promotion of healing in skin tissues damaged by bacterial infections. A hybrid hydrogel containing BP NSs was fabricated through straightforward electrostatic interactions. Within this hydrogel system, BP NSs efficiently produced $^1O_2$ when exposed to visible light, significantly bolstering their antibacterial efficacy against both Gram-positive and Gram-negative bacteria. Moreover, these BP NSs facilitated cellular proliferation and differentiation by activating the phosphoinositide 3-kinase/phosphorylation of protein kinase B (PI3K/Akt) and extracellular signal-regulated kinase (ERK1/2) signaling pathways. *In vivo* results revealed that BP NSs in this hybrid hydrogel could promote the formation of fibrinogen during the early stages of tissue reconstruction, thereby accelerating incrustation.[65] Additionally, Huang et al.[66] encapsulated BPQDs within a hydrogel (BPQDs@NH) composed of polyvinyl alcohol (PVA) and alginate sodium (Alg). This strategy was employed to efficiently clear methicillin-resistant *Staphylococcus aureus* (MRSA) from diabetic wounds, facilitating rapid healing. *In vitro* experiments showed that BPQDs@NH-guided synergistic PTT/PDT achieved an MRSA clearance rate of approximately 90%. Animal experiments revealed that BPQDs@NH reduced the inflammatory response by upregulating the expression of vascular endothelial growth factor (VEGF) and basic fibroblast growth factor (bFGF), ultimately leading to effective wound closure.

The tumor microenvironment (TME) is often characterized by hypoxia and acidity due to the rapid migration and proliferation of tumor cells.[69] For PDT induced by photosensitizers, the presence of oxygen is crucial for generating biotoxic ROS. Paradoxically, the consumption of oxygen during PDT exacerbates TME hypoxia, thereby limiting therapeutic effectiveness.[70] Consequently, strategies to modulate oxygen levels within the TME have gained widespread attention as a means to enhance PDT outcomes. In recent years, there has been growing interest in the decomposition of excessive hydrogen peroxide (H_2O_2) within the TME to provide a source of endogenous oxygen for PDT. This approach aims to alleviate the hypoxic and acidic conditions of the TME, thereby increasing the sensitivity of tumor cells to PDT. Liu et al.[71] developed a multifunctional nanoplatform by assembling rhodamine B-encapsulated manganese dioxide and peptide-functionalized BP NSs. This nanoplatform effectively catalyzed the decomposition of H_2O_2 in the TME using MnO_2, generating endogenous oxygen and consequently ameliorating local hypoxia at the tumor site. Thus, the increased oxygen pressure intensified PDT induced by BP NSs. Animal experiments demonstrated that this dual-modal imaging-guided

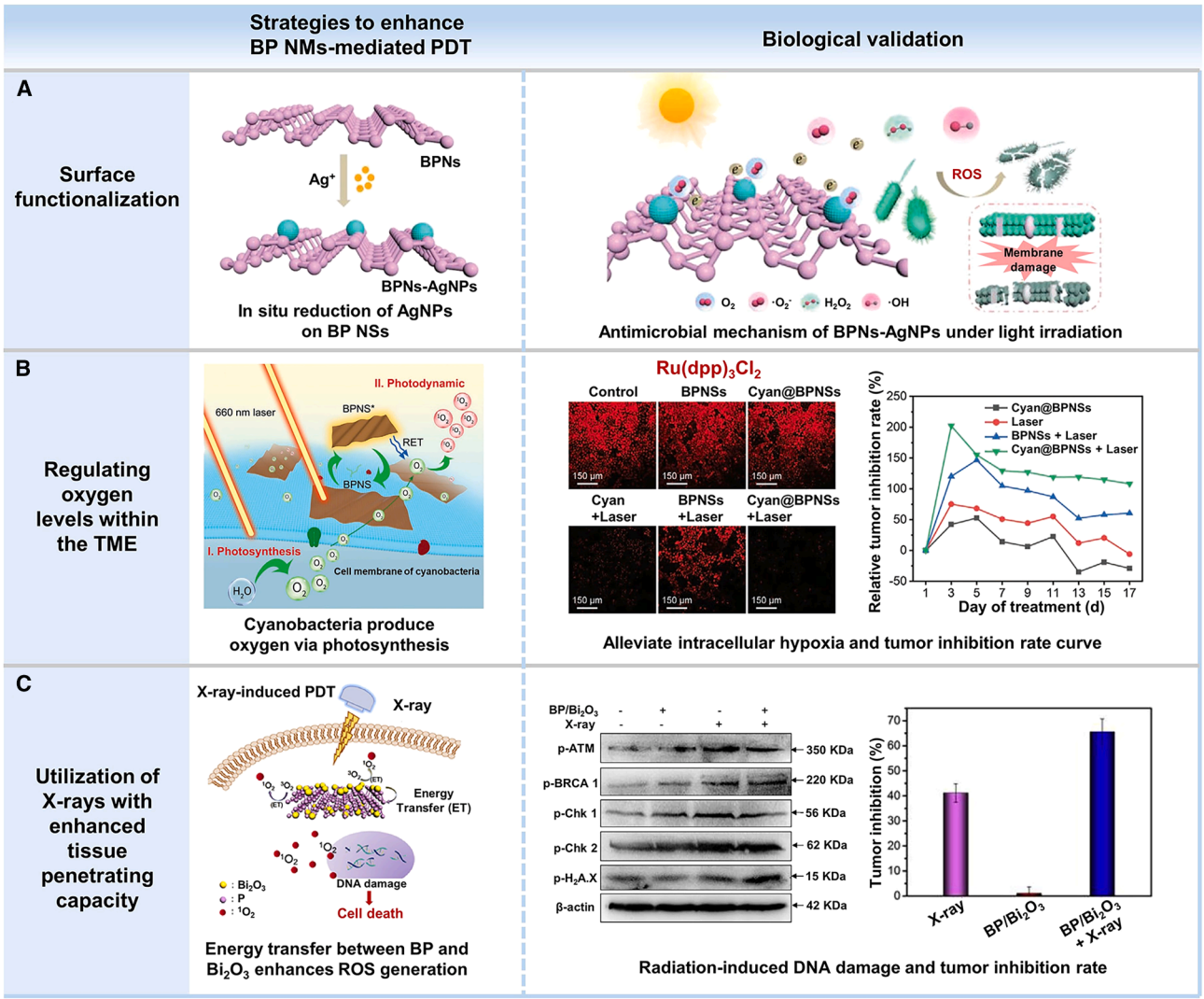

Figure 5. Strategies for enhancing BP NMs-mediated PDT

(A) Silver-laden BP NS for effective antibacterial treatment.[62] Copyright 2020, Wiley-VCH.

(B) Schematic illustration of Cyan@BP NSs enhancing PDT via photosynthesis.[67] Copyright 2021, Wiley-VCH.

(C) BP/Bi_2O_3-guided X-ray-PDT (n = 10).[68] Data are expressed as the mean ± SD. Copyright 2018, Elsevier.

therapeutic platform was highly effective in inhibiting tumor growth, with no significant recurrence observed.[72] Liu et al.[73] combined a heme dimer (dHeme) with FA-modified BP NSs (Cy5-dHeme-BPNS-FA) through noncovalent interactions. Leveraging the tumor-targeting ability of FA, specific aggregation of BP NSs at tumor sites could be achieved. Simultaneously, intracellular ATP was harnessed to break down dHeme within the nanoplatform into highly active monomeric 5′-cyanine-5 (Cy5)-conjugated aptamer-heme (H1) and 3′-heme-labeled oligonucleotide (H2). These constituents worked synergistically to continuously decompose endogenous H_2O_2 into O_2, thus augmenting the efficiency of BP-induced PDT. Lei et al.[74] encapsulated BPQDs and catalase in both the inner and outer layers of the metal-organic framework MIL-101 (BQ-MIL@cat-MIL) to yield a tandem catalytic reaction. The natural catalase encapsulated in BQ-MIL@cat-MIL could decompose excessive H_2O_2 in the TME into O_2. The generated O_2 was then directed to the inner layer, bolstering QD-induced PDT. Additionally, cyanobacteria, biocompatible photosynthetic prokaryotes, can serve as endogenous oxygen generators via photosynthesis. Their introduction into the TME has been shown to alleviate hypoxia and augment PDT efficacy. Qi et al.[67] developed a novel bioreactor, termed Cyan@BP NSs, which integrated microbial cyanobacteria with BP NSs. When subjected to 660 nm laser irradiation, the cyanobacteria continually produced endogenous oxygen via photosynthesis,[75] alleviating hypoxia at the tumor site. Thus, PDT triggered by BP NSs was significantly enhanced, achieving high-efficiency *in vivo* antitumor activity (Figure 5B).

In PDT, the generation of ROS by a photosensitizer through energy transfer upon light exposure is a crucial process.

However, in the absence of light, ROS generation efficiency is markedly reduced, rendering PDT therapeutically ineffective. Prolonged light exposure can also induce phototoxicity in cells, compounding this issue.[76] To address these challenges, Tian et al.[77] amalgamated poly(4-pyridonemethylstyrene) (PPMS) endoperoxide with BP NSs to create an intriguing film (PPMS-EPO/BPS), which functioned as a nanoplatform for ROS generation under light irradiation. Remarkably, it exhibited the unique capability of storing and controlling the release of ROS even in the absence of light. The PPMS-EPO/BPS film eliminated phototoxicity caused by long-term light exposure and imparted antibacterial properties to the photosensitizer even when not exposed to light, thereby enhancing its therapeutic potential.

BP-induced PDT is generally believed to be excited under red light illumination. However, the limited tissue penetration depth of red light constrains the application of BP in PDT. In stark contrast, the superior tissue penetration ability of X-rays offers significant advantages for deep tumor treatment.[78] Huang et al.[68] fabricated BP/Bi_2O_3 heterostructures by *in situ* growth of Bi_2O_3 NPs on BP NSs. Upon X-ray irradiation, Bi_2O_3 generated high-energy photoelectrons and low-energy Auger electrons, which decomposed surrounding water molecules to produce ROS.[79] Energy transfer between BP and Bi_2O_3 further amplified ROS generation efficiency. *In vivo* treatment outcomes validated the potential of X-ray-induced PDT to sensitize tumor cells to radiotherapy, effectively eliminating melanoma and suppressing further tumor growth (Figure 5C). Moreover, Chan et al.[80] harnessed unsaturated iridium complexes to occupy the lone pair electrons of BP NSs (RGD-Ir@BP), thereby enhancing their stability during treatment. The iridium complexes substantially enhanced the photocurrent response and photoinduced carrier dynamics of BP NSs.[81] Under X-ray exposure, the RGD-Ir@BP nanoplatform reduced prostaglandin E2 levels and exhibited excellent ROS generation efficiency. The synergistic strategy proved highly effective in eradicating nasopharyngeal carcinoma tumors.

Bioregulation based on the sonodynamic effect and piezoelectric effect of BP

Owing to its unique semiconductor properties, strong directionality, and non-centrosymmetric lattice structure, BP can efficiently generate ROS under US stimulation through combined sonochemical and piezoelectric effects, enabling noninvasive treatment of deep tissues. Its pronounced piezoelectric response further allows the generation of a stable electric potential under mechanical stress, thereby driving redox reactions or modulating cellular electrical signaling, endowing BP with considerable potential for piezoelectric therapy. SDT offers notable advantages, including minimal invasiveness, low systemic toxicity, and excellent penetration into deep-seated tissues. Li et al.[82] employed BP NSs as sonosensitizers for tumor therapy and elucidated the mechanism of ROS generation through US-induced piezoelectric polarization. *In vitro* and *in vivo* studies confirmed significant tumor suppression without discernible adverse effects. In addition to their use as standalone sonosensitizers, BP NSs can be covalently modified to further amplify SDT performance, thereby enabling more effective treatment of deep tumors. Liu et al.[83] demonstrated that BP NSs could serve as sonosensitizers, capable of generating hydroxyl radicals (·OH) when exposed to US. Furthermore, to enhance the stability of BP NSs, three distinct covalently modified BP NS structures were synthesized: C60 modification at the edge (C60-e-BP) and surface (C60-*s*-BP), as well as modification with benzoic acid (BA-*s*-BP). Systematic investigations into the SDT efficiencies of these covalently modified BP NSs unveiled that both C60-*s*-BP and BA-*s*-BP outperformed unmodified BP NSs, with BA-*s*-BP exhibiting the best effect. In addition to covalent modification, the incorporation of metal NPs onto the surface of BP nanomaterials can significantly amplify the BP-induced SDT effect. Chen et al.[84] engineered BP NSs by anchoring gold NPs (Au NPs), MnO_2, and soybean phospholipids to establish a novel sono-activated tumor therapy platform (Au/BP@MS). Here, Au NPs effectively curbed the rapid recombination of electron-hole pairs in BP NSs, optimizing the SDT effect. Additionally, the MnO_2 coating on BP NSs facilitated the consumption of a substantial quantity of H_2O_2 within tumor cells, generating endogenous O_2 while simultaneously depleting intracellular glutathione (GSH). This dual-action approach augmented the effectiveness of SDT. Leveraging BP's piezoelectric properties, Jia et al.[85] designed a decellularized adipose tissue (DAT)-based PDA-mBP@DAT composite scaffold integrating the photothermal property of PDA and the piezoelectricity of multilayer BP NSs (mBP). This scaffold synergistically promoted bone regeneration through multiple physical cues (US, heat, and electricity). Under low-intensity pulsed US (LIPUS) stimulation, the scaffold accelerated bone tissue repair by promoting angiogenesis and activating Piezo1.

Combination therapy

Due to their large specific surface area, BP can serve as excellent drug carriers, offering a promising strategy for integrating small-molecule chemotherapy with PTT. This dual functionality not only maximizes therapeutic outcomes but also minimizes side effects, paving the way for innovative and effective cancer therapies. Wu et al.[86] developed a BP NSs-based drug delivery system by conjugating phenethyl isothiocyanate (PEITC), a compound capable of selectively targeting mutant p53 in tumor cells. This strategy significantly enhanced cellular sensitivity to the chemotherapeutic agent doxorubicin (DOX) and effectively reversed multiple drug resistance. Moreover, the synergistic combination of BP-mediated phototherapy and chemotherapy resulted in efficient inhibition of drug-resistant tumor growth (Figure 6A).

PTT alone often faces challenges such as restricted tissue penetration of NIR light and insufficient accumulation of photothermal agents within tumors, which constrain its efficacy.[89] Combining PTT with other therapeutic approaches has therefore become an effective strategy to overcome these limitations.[90,91] For example, Hu et al.[87] developed a multifunctional platform (BP@Cu) by leveraging the lone-pair electrons on BP to capture Cu^{2+} ions. The Cu^{2+} shell augments the stability of BP NSs while simultaneously improving their photothermal performance. Moreover, Cu^{+}/Cu^{2+} species catalyze Fenton-like reactions with H_2O_2 in the TME, producing highly cytotoxic ·OH, thereby achieving a synergistic effect between chemodynamic therapy (CDT) and PTT (Figure 6B). Zhao et al.[92] designed a cooperative platform (BPN-MnCO) by coordinating BP NSs with metal carbonyl complexes. Upon irradiation, MnCO underwent

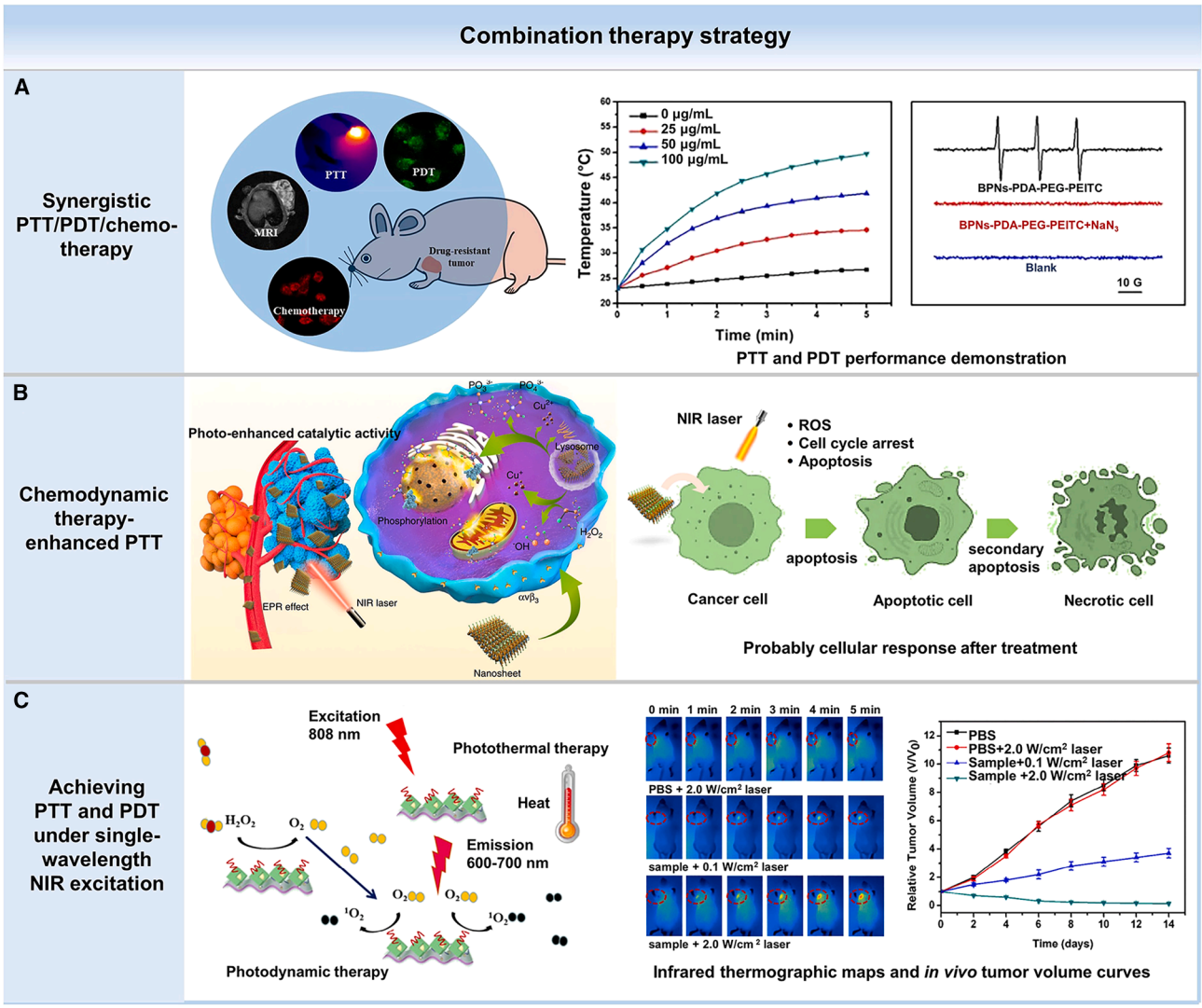

Figure 6. Combination therapy strategies based on BP NMs

(A) The multifunctional nanoplatform BPNs-PDA-PEG-PEITC-Mn/DOX enables bioimaging-guided cancer therapy.[86] Copyright 2019, Elsevier.

(B) BP@Cu multifunctional nanotherapeutic platform.[87] Copyright 2020, Springer Nature.

(C) MUCNPs@BPNS-Ce6 nanoplatforms-induced synergistic PDT and PTT treatment under 808 nm laser irradiation (n = 3).[88] Copyright 2020, Elsevier.

photodegradation to release endogenous carbon monoxide (CO). The photothermal properties of BP facilitated localized heating, which not only enhanced CO-induced DNA damage but also suppressed its repair, thereby activating the ATM-GADD45-p53-Cyclin B cell death pathway to promote apoptosis.

Hypoxia within the TME continues to pose a critical challenge to effective PDT.[93] However, combining PTT and PDT has shown potential in overcoming this restriction. Heat generated by PTT improves tumor oxygenation by bolstering local blood flow, thereby augmenting PDT efficacy. Conversely, PDT can sustain hypoxic and acidic conditions at tumor sites, sensitizing cells to subsequent PTT.[94] When a single nanomaterial can simultaneously perform PTT and PDT, the therapeutic system is simplified while maximizing therapeutic output. Chen et al.[95] exploited the large surface area and distinctive electronic structure of BP to construct an integrated platform combining PTT, PDT, and chemotherapy. Local hyperthermia induced by PTT increases membrane permeability and boosts drug uptake at tumor sites while also directly damaging tumor tissue. Meanwhile, PDT-generated singlet $^1O_2$ causes oxidative damage to intracellular organelles, triggering oxidative stress.[96] Both *in vitro* and *in vivo* studies confirmed that this trimodal therapeutic platform outperformed single and dual therapy strategies in tumor ablation and suppression.

Multimodal phototherapy for cancer treatment typically requires simultaneous irradiation with multiple wavelengths,[97] presenting considerable practical challenges for the application of BP nanomaterials. Furthermore, the limited tissue penetration of visible light commonly used in PDT, compared to NIR light,

further complicates therapeutic procedures. To address this, strategies enabling both PTT and PDT under single-wavelength NIR excitation are in urgent demand. Lin et al.[98] addressed this challenge by integrating upconversion NPs (UCNPs) with BP NSs, facilitating NIR-triggered BP-mediated PDT. Similarly, Zhang et al.[88] designed a multifunctional nanoplatform, MUCNPs@BPNS-Ce6, by loading UCNPs and the photosensitizer chlorin e6 (Ce6) onto Fe_3O_4@MnO_2 NPs, which were subsequently assembled onto poly-L-lysine (PL)-modified BP NSs. The PL modification enhanced the physiological stability of BP NSs and functioned as a multifunctional linker for efficient material integration. This composite platform enabled PTT/PDT activation by a single NIR wavelength, while the UCNPs converted NIR light into specific wavelengths to trigger both BP and Ce6-mediated PDT.[99] Simultaneously, MnO_2 catalyzed the conversion of endogenous H_2O_2 into oxygen, alleviating tumor hypoxia and further enhancing PDT efficacy.[100] Guided by dual-modal MRI and fluorescence (FL) imaging, the nanoplatform demonstrated potent antitumor activity both *in vitro* and *in vivo* (Figure 6C).

Redox regulation strategy based on the reduction properties of BP

BP contains phosphorus atoms with unbonded lone electron pairs that exhibit high reactivity under physiological conditions. These electrons enable BP to act as an effective electron donor in redox reactions, facilitating ROS scavenging and the regulation of cellular redox homeostasis. Additionally, through cation-π interactions, BP can form P-M coordination bonds with metal cations, enabling the *in situ* sequestration of metal ions. These properties render BP NMs promising for diverse biomedical applications, encompassing antioxidant therapy, intervention in metal-related disorders, tissue regeneration, and neuroprotection.

BP acts as a reducing agent to directly scavenge ROS

Accumulating evidence has linked elevated ROS levels to the pathogenesis of various diseases, including acute kidney injury, osteoarthritis, intervertebral disc degeneration, and Parkinson's disease. Excessive ROS accumulation can induce oxidative stress, disrupt cellular structures and functions, and ultimately trigger apoptosis. Thus, the effective elimination of ROS holds significant therapeutic potential. Owing to its unique electronic structure and high chemical reactivity, BP has emerged as a promising antioxidant NM capable of efficiently scavenging excess ROS *in vivo*. Hou et al.[18] demonstrated that BP preferentially accumulated in the kidneys, likely due to the structural similarity between its layered architecture and that of sheet-like DNA. Further studies revealed that BP NSs, as an antioxidant nanoplatform, efficiently eliminated renal ROS *in vivo* and markedly mitigated oxidative stress-induced apoptosis, underscoring their potential in the treatment of ROS-related pathologies. In addition, Ge et al.[101] developed novel BPQD nanoprobes for NIR-II FL imaging-guided therapy. These nanoprobes exhibited excellent biodegradability and tunable optical properties, selectively accumulating in the kidney and liver, where they effectively scavenged ROS. Low doses of BPQDs could protect tissues from ROS-mediated acute kidney and liver injuries while being monitored through responsive NIR-II FL imaging.

Additionally, elevated ROS levels perturb the brain's microenvironment homeostasis, thereby facilitating the development of Parkinson's disease. Nevertheless, effective drug penetration through the blood-brain barrier (BBB) poses obstacles to therapeutic intervention. Leveraging BP's photothermal effect to facilitate BBB penetration, together with its ROS-scavenging and delivery capabilities, Cheng et al.[102] developed a nanodelivery platform for remodeling the brain microenvironment. This platform cleared excessive ROS, reduced neuroinflammation, inhibited pathogenic proteins, facilitated neurotransmitter recovery, and ultimately elevated dopamine levels. Moreover, BP NSs are also used in osteoarthritis treatment. Recent research indicated that BP NSs maintained the balance between cartilage matrix anabolism and catabolism by eliminating intracellular ROS, thereby facilitating cartilage protection and subchondral bone repair.[103] To alleviate extracellular acidosis in the nucleus pulposus, block inflammatory cascades, reduce matrix metalloproteinase (MMP) expression, and remodel the intervertebral disc extracellular matrix (ECM) in intervertebral disc degeneration, Li et al.[104] designed novel oxygen metabolism-balanced engineered BP hydrogel microspheres, which could reduce H_2O_2 intensity by 229%, restore tissue function, and promote nucleus pulposus regeneration. In addition, He et al.[105] developed a targeted nanotherapeutic platform based on BP NSs (BPNSs@PEG-S2P/R). This platform employed BP NSs as a drug carrier while harnessing their intrinsic antioxidant and anti-inflammatory activity. It could efficiently remove various types of ROS and inhibit the expression of proinflammatory factors associated with atherosclerosis in pathological macrophages. The incorporation of a targeting peptide (S2P) and ROS-responsive drug release enabled site-specific delivery and promoted local drug accumulation, thereby minimizing systemic side effects. Notably, BPNSs@PEG-S2P/R demonstrated robust therapeutic efficacy across multiple atherosclerosis models, with high reproducibility and model independence, underscoring its broad translational potential (Figure 7).

BP indirectly intervenes in oxidative stress caused by metal dyshomeostasis by capturing metal ions

Owing to the high reactivity of the lone pair electrons and edge-dangling bonds of surface phosphorus atoms, BP can selectively bind metal ions *in vivo*, serving as a reduction center. Elevated levels of transition metal ions in cells are recognized as key pathogenic factors in the onset and progression of neurodegenerative diseases.[106] For instance, copper dyshomeostasis has been closely linked to oxidative stress and neuronal apoptosis.[107] Through selective binding to dysregulated metal ions, BP NSs can mitigate metal-induced excessive ROS generation, underscoring their potential in neuroprotection. Furthermore, the BBB remains a major challenge for drug delivery to the central nervous system. Benefiting from their photothermal properties, BP NSs exhibited optimized BBB permeability under NIR irradiation, enabling precise therapeutic intervention in brain disorders (Figure 8A).[108]

Wilson disease (WD), a hereditary disorder of copper metabolism, is characterized by the pathological accumulation of copper ions, particularly in the liver and brain.[110] To address this, Kim et al.[109] developed a hyaluronate-diaminohexane/BP (HA–DAH/BP) complex as a copper-specific chelator for

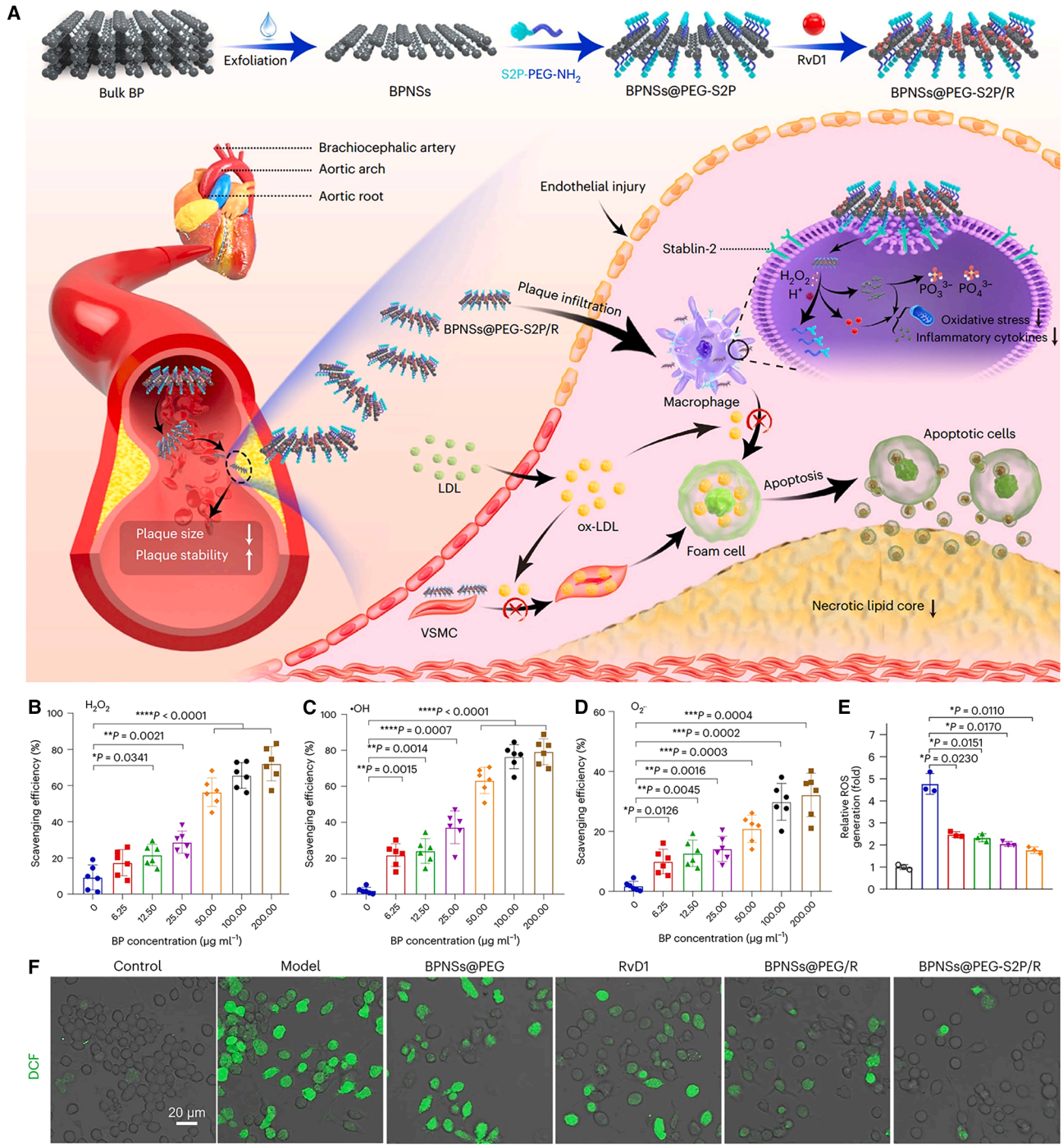

Figure 7. BP NMs as antioxidants for synergistic therapy

(A) Schematic of the synthesis and anti-atherosclerotic mechanism of BPNSs@PEG-S2P/R.

(B–D) Scavenging capability of BPNSs@PEG-S2P toward ROS (n = 6).

(E and F) Representative fluorescence microscopy images of intracellular ROS generation in RAW264.7 cells treated with different formulations, accompanied by corresponding flow cytometry quantification (n = 3).[105] Data are expressed as the mean ± SD. Copyright 2024, Springer Nature.

captured hepatic Cu^{2+}. This nanocomposite demonstrated broad-spectrum chelating capability, effectively binding Ca^{2+}, Mg^{2+}, Fe^{2+}, Cu^{2+}, and Zn^{2+} ions. Moreover, HA-DAH/BP exhibited good biocompatibility in HepG2 liver cancer cells. The incorporation of HA enhanced the stability of BP NSs, prevented rapid *in vivo* degradation, and facilitated liver-specific targeting,

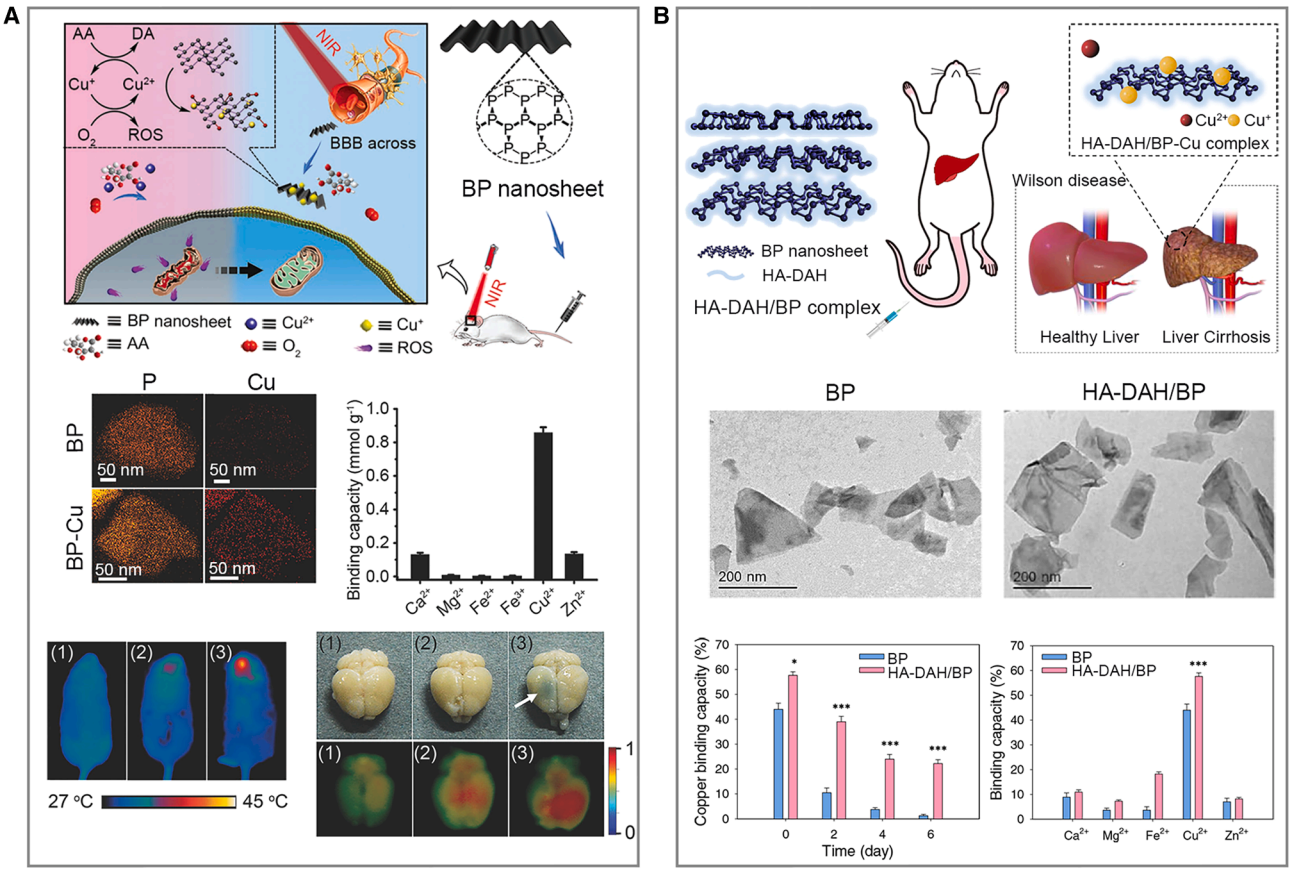

Figure 8. BP NMs regulate oxidative stress by capturing metal ions

(A) BP NSs mitigate oxidative stress in neurodegenerative therapy by crossing the BBB and capturing Cu^{2+}. (1) BP, (2) NIR, (3) BP + NIR.[108] Copyright 2018, Wiley-VCH.

(B) HA-DAH/BP complexes remove accumulated Cu^{2+} in the liver for WD treatment (n = 3).[109] Copyright 2021, Springer Nature.

significantly improving Cu^{2+} capturing efficiency. Nonetheless, further validation in animal models is required to advance the clinical translation of this strategy for WD treatment (Figure 8B).

Biological effects of BP metabolites and intermediates

The surface phosphorus atoms of BP, bearing lone electron pairs and edge unsaturated bonds, confer pronounced chemical reactivity while rendering the material highly susceptible to water and oxygen, leading to rapid degradation under physiological conditions. This degradation is coupled with redox processes that perturb the local microenvironment, disrupt cellular EM and redox homeostasis, and induce oxidative stress, mitochondrial dysfunction, and apoptosis in tumor tissues, thereby exerting potent antitumor effects.[111] Concurrently, the resulting PO_4^{3-}, as physiologically relevant metabolites, participates in essential biological processes, including bone mineralization, ATP production, and nucleic acid synthesis, while promoting osteogenesis, angiogenesis, and neural regeneration, positioning BP as a multifunctional platform for both tumor therapy and tissue engineering.

Regulation of ionic homeostasis by BP metabolites

In the presence of endogenous water and oxygen, BP nanomaterials spontaneously degrade, rapidly releasing PO_4^{3-} into the cellular microenvironment. This leads to a sharp increase in local ion concentration and a pH shift, potentially disturbing cellular homeostasis, inducing oxidative stress and mitochondrial dysfunction, and ultimately triggering irreversible cell damage and apoptosis.[112] This degradation property lays the foundation for its bioactive applications while also necessitating attention to dose-dependent effects.

In antitumor therapy, the PO_4^{3-} released during BP degradation confers pronounced selective cytotoxicity. Zhou et al.[113] demonstrated that BP NSs possess intrinsic anticancer activity. Owing to the stronger oxidative stress and accelerated metabolism characteristic of tumor cells, BP undergoes markedly faster biodegradation in tumor cells than in normal cells, leading to substantial phosphate release with minimal impact on healthy tissues. This selective degradation arrests cancer cells at the G2/M phase and triggers robust apoptosis and autophagic cell death. Although apoptosis inhibitors (Z-VAD-fmk) and autophagy inhibitors (3-methyladenine, 3-MA) partially mitigate cell death, neither restores viability, indicating that BP-mediated cytotoxicity is predominantly driven by cell cycle-dependent apoptosis and autophagy (Figure 9A). Moreover, Kong et al.[114] further identified a concentration-dependent "selective killing"

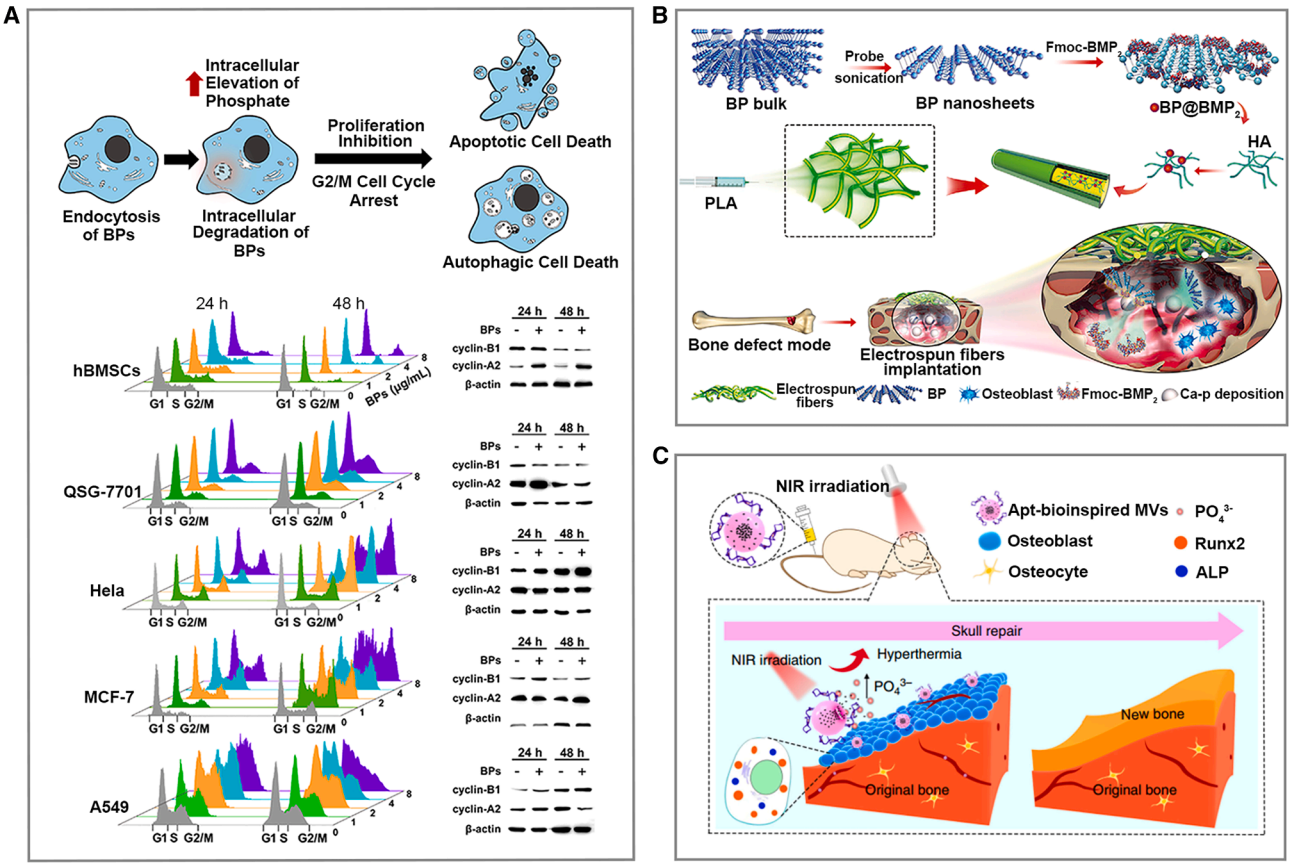

Figure 9. Biological activities of BP metabolites and intermediates

(A) BP induces cell-cycle arrest at the G2/M phase and triggers cell death through apoptosis and autophagy.[113] Copyright 2019, Wiley-VCH.

(B) BP@BMP2 scaffolds recruit osteoblasts and release calcium-free phosphate to promote bone physiological regeneration *in vivo*.[115] Copyright 2020, Wiley-VCH.

(C) Apt-bioinspired MVs in cell mineralization. ALP, alkaline phosphatase; Runx2, runt-related transcription factor 2.[116] Copyright 2019, Springer Nature.

(SK) window, within which BP NSs induce high levels of ROS in cancer cells while sparing normal cells. Elevated ROS disrupted the cytoskeleton, blocked cell cycle progression, induced DNA damage, and activated apoptotic pathways. Additionally, ROS accumulation promoted lipid peroxidation and suppressed superoxide dismutase (SOD) activity, amplifying oxidative stress. However, exceeding the SK range may result in off-target toxicity, highlighting the need for precise dose control.

Based on the degradation properties and bioactivity of BP, researchers have developed various functionalized nanotherapeutic systems. According to the Brønsted-Lowry acid-base theory, the hydrolysis of phosphate ions consumes protons (H^+) and raises the local pH, potentially enhancing the therapeutic efficacy of BP. Pan et al.[117] developed a biomineralization strategy to functionalize BP NSs with *in situ* calcium phosphate (CaP) coatings, generating CaBPs with enhanced physiological stability. The pH-sensitive degradation of CaBPs was accelerated in the acidic TME, enabling controlled release of PO_4^{3-}. CaBPs selectively targeted mitochondria, disrupted their membrane integrity, and initiated mitochondria-dependent apoptosis, demonstrating robust tumor growth inhibition. Moreover, Yang et al.[118] reported that BP NSs acted as autophagy inhibitors. When combined with anti-glycolytic agents, they effectively blocked both aerobic glycolysis and autophagy-dependent metabolic pathways, resulting in synergistic tumor inhibition.

BP metabolites participate in tissue regeneration

Owing to its unique degradability and biologically favorable degradation products, BP exhibits remarkable potential in tissue engineering. Under physiological conditions, it gradually breaks down into non-toxic PO_4^{3-}, thereby circumventing biosafety concerns while simultaneously promoting key regenerative processes such as osteogenesis and angiogenesis. Furthermore, the highly tunable surface characteristics and distinctive physicochemical properties of BP contribute to its multifunctionality. These attributes collectively position BP NMs as promising platforms for applications in regenerative medicine, including bone repair and neural tissue regeneration.

Biodegradable BP nanomaterials enable the sustained release of PO_4^{3-}, a critical inorganic component for the synthesis of hydroxyapatite (HA), thereby facilitating bone tissue mineralization. PO_4^{3-} readily binds with Ca^{2+} to induce the rapid nucleation of CaP nanocrystals, significantly enhancing mineralization.

Leveraging the excellent biocompatibility and osteoinductive properties of BP, researchers developed an ultrathin BP nanodots coating that provided a favorable microenvironment for the proliferation and spontaneous osteogenic differentiation of MC3T3-E1 pre-osteoblasts.[119] To mimic the ECM and further support tissue regeneration, BP NSs were incorporated into double-network nanoengineered (NE) hydrogels. These BP-integrated hydrogels exhibited accelerated CaP crystal formation, improved mineralization capacity, augmented mechanical strength, and increased bioactivity. It is also critical to note that BP NSs embedded within NE hydrogels acted synergistically with CaP *in vivo* to significantly promote skull bone regeneration.[120] Taking advantage of the negatively charged BP surface, BP was also employed as a delivery vehicle for BMP-2, enabling the recruitment of osteoblast precursor cells and their osteogenic differentiation. Based on this strategy, a BP@BMP-2-loaded electrospun fiber scaffold was developed, which effectively facilitated osteoblast migration and differentiation while accelerating ECM mineralization (Figure 9B).[115]

With physiologically favorable degradation products and superior photothermal conversion efficiency, BP emerges as a promising candidate for developing advanced therapeutic strategies in tissue engineering. Notably, BPs@PLGA composites maintained robust NIR photothermal responsiveness even under 7 mm of tissue coverage, effectively upregulating HSP expression and further enhancing osteogenesis.[121] Matrix vesicles (MVs), specialized EVs secreted by bone-related cells, play a crucial role in regulating bone mineralization.[122] Combining the advantages of BPQDs and MVs, Wang et al.[116] designed an aptamer-guided, bioinspired MV system that significantly stimulated *in vivo* bone regeneration in a mouse skull defect model (Figure 9C). Building on BP's photoresponsiveness, Shao et al.[123] developed a BP@Hydrogel system exhibiting NIR-controlled biomineralization. As mineralization is dependent on PO_4^{3-} concentration, this platform allows precise spatial and temporal regulation of bone regeneration via light modulation.

The multifunctionality of BP confers distinct advantages in treating infected bone defects. Its degradability ensures sustained phosphate release, while its intrinsic photothermal antibacterial properties and ability to modulate cellular behavior enable concurrent infection control and bone regeneration. Moreover, it has been demonstrated that BP has a stimulatory effect on angiogenesis and neurogenesis, further broadening its therapeutic potential in complex bone defect repair. For instance, a magnesium-doped BP/GelMA composite hydrogel (GelMA-BP@Mg), developed by Jing et al.,[124] exhibited potent osteoinductive capacity, strong antibacterial effects, and the ability to promote early-stage vascularization and neurogenesis in a rat skull defect model, ultimately enhancing bone regeneration and remodeling.[125] Similarly, a BP-functionalized electrospun scaffold, developed by Li et al.,[126] provided both phosphorus supplementation and photothermal support, synergistically promoting bone regeneration. In a scaffold fabricated via microfluidic 3D printing, BP NSs not only improved *in situ* mineralization but also promoted vascular growth, thereby facilitating the formation of large blood vessels within the defect core and significantly accelerating bone repair under NIR irradiation.[127] Tao et al.[128] engineered a multifunctional bone-repair scaffold by integrating BP NSs into polycaprolactone nanofibers, thereby endowing the construct with robust NIR photothermal responsiveness. Surface functionalization with the MSC-specific aptamer Apt19S enabled active recruitment of endogenous MSCs, while phase-change material microspheres deposited on the scaffold provided mild-photothermal-triggered, on-demand antibiotic release for effective infection control. Upon NIR irradiation, the mild photothermal effect upregulated HSP, accelerated BP NSs degradation and the consequent release of osteogenic PO_4^{3-}, and markedly enhanced MSC osteogenic differentiation and biomineralization. Both *in vitro* and *in vivo* studies demonstrate that this biomimetic, photothermally reinforced scaffold synergistically achieves antibacterial activity, stem cell recruitment, and bone regeneration, highlighting its strong potential for therapeutic repair of bone defects.

BP intervenes in basic cellular life activities by directly binding to biomolecules or organelles

The bioactivity of BP NMs emerges from their ability to engage in both specific and non-specific, multi-level interactions with cellular components, positioning them not merely as passive carriers but as active participants in biological regulation. Through direct binding to proteins, membranes, and organelles, BP nanomaterials influence fundamental processes, including signal transduction, EM, and cell fate decisions. The effectiveness of these biological functions derives from their intrinsic redox activity, tunable surface properties, and high affinity for biological structures, thus enabling precise intervention in pathological mechanisms via two distinct interaction modes: non-specific interactions mediated primarily by van der Waals forces and electrostatic interactions, typified by protein corona formation and α-synuclein fibril disaggregation; and specific interactions involving targeted binding to intracellular proteins through structural complementarity, hydrogen bonding, and synergistic electrostatic attraction, such as selective binding to functional domains of key regulatory proteins for precise functional modulation.

The formation of nanomaterial-protein corona complexes significantly influences the *in vivo* immune responses to NMs, underscoring the necessity of exploring the interplay between BP NMs and their biomolecular corona. Upon entering biological environments, BP NMs rapidly adsorb plasma proteins to form a dynamic corona that determines their subsequent biological behavior. As demonstrated by Mo et al.,[7] the composition of the corona depends on BP size, protein concentration, and molecular weight. Liquid chromatography-tandem mass spectrometry (LC-MS/MS) analysis revealed preferential adsorption of negatively charged proteins, indicating that while electrostatic attraction plays a role, it is only one aspect of a complex binding process that also involves hydrophobic interactions and structural complementarity. This protein layer confers a context-dependent biological identity, influencing cellular uptake mechanisms and immune responses. Specifically, the BP-protein corona activated the NF-κB pathway and induced immune perturbations in macrophages, demonstrating how the surface biointerface governs nanomaterial-immune system crosstalk.

BP nanomaterials also function via direct physical interactions with pathogenic biomolecular assemblies. For example, in

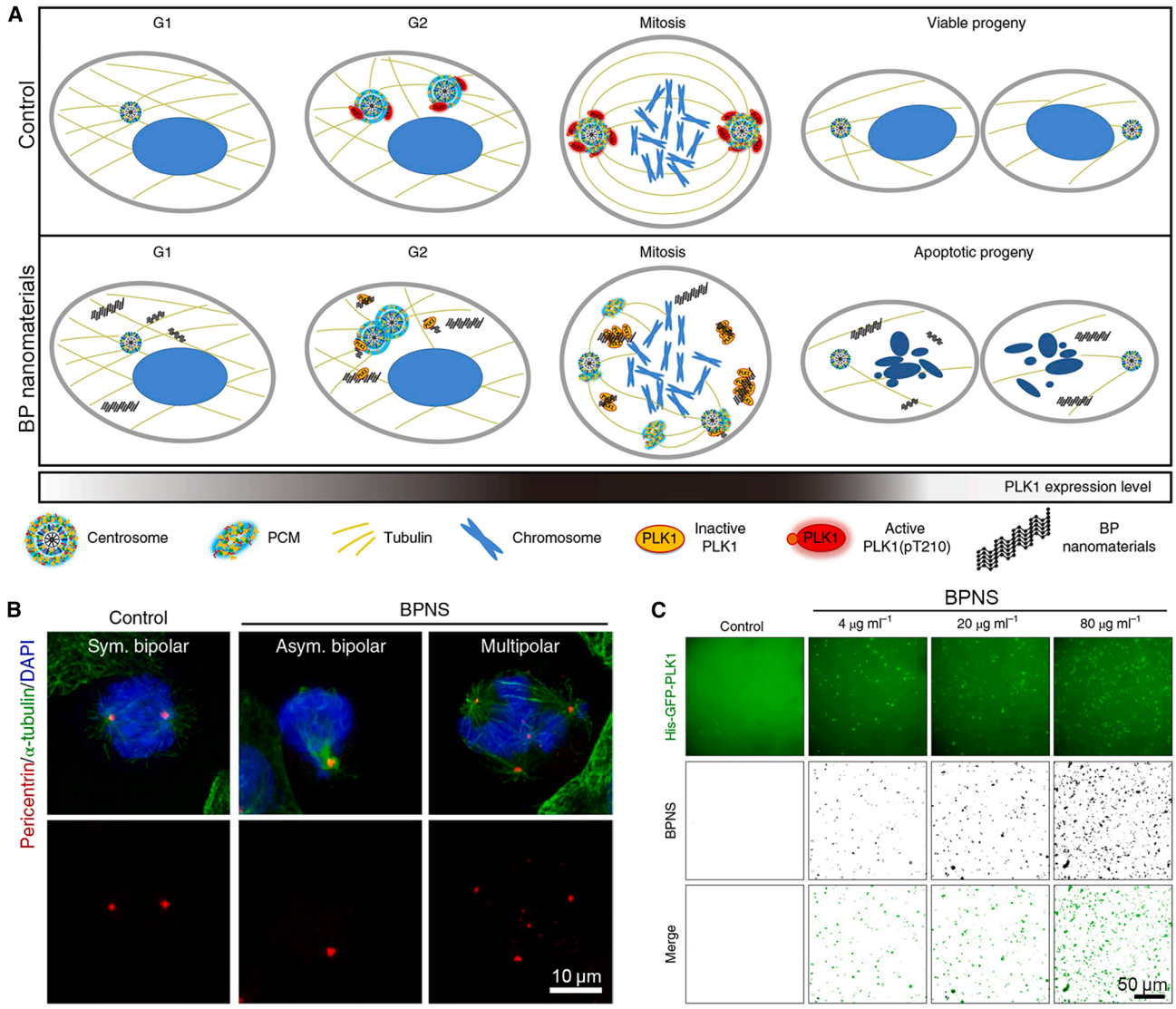

Figure 10. BP regulates mitotic progression by directly interacting with biomolecules

(A) Mechanism of BP nanomaterials' effects on the cell cycle.

(B) Coimmunostaining of α-tubulin and pericardial material in HeLa cells treated with BP NSs.

(C) Aggregation of purified His-GFP-PLK1 protein after treatment with BP NSs *in vitro*.[131] Copyright 2021, Springer Nature.

models of Parkinson's disease, BP NSs employ van der Waals forces to directly disaggregate α-synuclein fibrils while concurrently activating autophagic clearance pathways. This dual-action strategy effectively diminishes pathological protein aggregation, rescues mitochondrial dysfunction, and attenuates neuronal damage.[129] It is worth noting that BP NSs have been proven to successfully cross the BBB in multiple Parkinson's disease mouse models, where they protect dopaminergic neurons and improve motor function, underscoring their potential as multifunctional neuroprotective agents.

To gain deeper insights into the specific biological interactions of BP NMs, a thorough understanding of their cellular uptake mechanisms is essential. Tao et al.[31] demonstrated that BP NSs first interact with the cell membrane. Using fluorescein isothiocyanate (FITC)-labeled BP NSs,[130] their study revealed that BP NSs are primarily internalized by cells through caveolae-dependent endocytosis and macropinocytosis, ultimately entering cells via lysosomes. Beyond initial cellular internalization, the high reactivity of BP nanomaterials enables direct interactions with cellular components, resulting in the inactivation or aggregation of specific bioactive molecules and thereby influencing fundamental cellular processes. A prominent example is their ability to disrupt mitotic progression by targeting centrosome integrity and key regulatory proteins. As demonstrated by Shao et al.,[131] BP NSs selectively bound to both the N-terminal kinase domain and the C-terminal Polo-box domain of Polo-like kinase 1 (PLK1), significantly impairing its cytoplasmic dynamics and function (Figure 10). This interaction led to the

accumulation of inactive PLK1 around the centrosome, reduced the cohesion of pericentriolar material (PCM), and promoted the formation of multipolar spindles during mitosis. Consequently, these disruptions result in mitotic delay or arrest, ultimately triggering apoptosis in cancer cells. Through these mechanisms, BP nanomaterials effectively targeted cell cycle regulation and demonstrated high selectivity toward malignant cells.

Furthermore, BP can directly interact with key biomolecules, such as immune-related receptors or signaling proteins, to actively modulate critical cellular pathways and influence immune cell function. For instance, by binding to HSP-90, BP induces autophagic degradation of programmed death ligand 1 (PD-L1) while concurrently suppressing PI3K-AKT signaling to inhibit PD-L1 transcription. This dual mechanism cooperatively alleviates immunosuppression in glioblastoma models, underscoring the potential of BP as an immune-sensitizing agent via direct interference with immune regulatory pathways.[132] As phosphate group donors, BPQDs@HSA directly bind to phosphatidylinositol-4-phosphate 5-kinase type 1 alpha (PIP5K1A), activating the PI3K-Akt-mTOR signaling pathway. This activation reprograms natural killer (NK) cell glycolytic metabolism and further promotes oxidative phosphorylation, thereby enhancing their metabolic activity and persistence. Additionally, BPQDs@HSA can interact with toll-like receptors (TLRs) on the surface of NK cells, increasing mTOR expression and activating the downstream NF-κB signaling pathway to regulate cytokine secretion and enhance immune tumoricidal activity. These findings demonstrate the ability of BP-based nanomaterials to directly engage with key biomolecules and orchestrate essential immune-metabolic processes.[133]

In addition to their direct interactions with biomolecules, BP nanomaterials exhibit biomimetic properties that enable metabolic intervention. In our study,[134] ultrasmall BPQDs were used as precursors to develop EM-engaged NMs (EM-eNMs). Through contact electrocatalysis, these BPQDs underwent selective surface oxidation, enabling precise targeting of metabolic processes. This strategy was informed by a structural and functional understanding of ATPase, allowing direct engagement with energy-related organellar systems to modulate essential cellular activities. As an analog of hydrated phosphate, EM-eNMs were recognized by MSCs as substrates for ATP synthesis and entered the mitochondrial inner membrane to directly regulate EM, thereby changing the mitochondrial morphology from reticular to rod-shaped and driving mitochondrial fission and mitophagy. Mechanistically, we demonstrated that EM-eNMs selectively bound to ATP5B and caused reversible aggregation of the ATP5B protein, which is linked to energy deficiency associated with aging. In a senile osteoporosis mouse model, bone mineral density increased approximately 3-fold after treatment with EM-eNMs, effectively reversing senile osteoporosis. Bone marrow MSCs (BMMSCs) isolated from the femurs of treated mice exhibited upregulated stemness and mitophagy, suggesting that the increase in bone mineral density was attributable to the effect of EM-eNMs on enhancing the stemness and functionality of BMMSCs, rather than a direct interaction with calcium to promote bone formation (Figure 11).

Collectively, these studies illustrate that BP NMs facilitate targeted therapeutic outcomes across neurological, oncological, and immunological contexts through diverse yet direct mechanisms, including specific biomolecular binding, physical interactions, and organelle-level intervention. By directly interacting with biomolecules and organelles, BP NMs enable precise modulation of fundamental cellular processes, demonstrating considerable versatility and establishing a promising platform for next-generation NMs.

Immunomodulatory function of BP

Recent studies increasingly highlight the immunomodulatory potential of BP NMs, demonstrating their capacity to reshape the immune microenvironment and trigger specific immune responses. The diverse immunological effects elicited by BP NMs arise from their unique physicochemical attributes—including thickness-dependent bandgap tunability, strong photothermal and photodynamic responsiveness, high surface reactivity, and intrinsic biodegradability—all of which collectively define their immune-related functionality. These properties are mechanistically linked to distinct immunological outcomes. For example, the high photothermal conversion efficiency and photoinduced ROS generation of BP can drive immunogenic cell death (ICD), promoting DC maturation and enhancing cytotoxic T cell infiltration. Its highly reactive surface facilitates interactions with macrophages and DCs, modulating cytokine secretion and strengthening antigen presentation. In addition, the gradual degradation of BP into phosphate alters the local ionic and redox milieu, further shaping immune responses. Together, these property-function relationships elucidate how BP NMs engage specific immune pathways and underscore their promise as rationally designable platforms for immunomodulation and immunotherapy.

BP NMs modulate the immune microenvironment by triggering ICD

The immunomodulatory effects of BP NMs are intrinsically associated with their ability to elicit ICD, a form of regulated cell death that activates adaptive immunity through the release of damage-associated molecular patterns (DAMPs) and tumor-associated antigens. Leveraging their unique photophysical properties and surface reactivity, BP nanomaterials facilitate ICD through multiple pathways, including PTT and PDT. These processes ultimately promote DC maturation, enhance infiltration of cytotoxic T lymphocytes (CTLs), and contribute to the reversal of immunosuppressive TME.[135]

The photothermal effect is the central pathway through which BP nanomaterials elicit ICD, where the nanomaterials absorb NIR light energy and convert it into thermal energy, resulting in localized hyperthermia. This localized heating triggers a series of cellular stress responses, including the release of DAMPs and the activation of HSPs, which collectively promote the immune system's recognition and elimination of cancerous cells. For instance, Ou et al.[136] developed a BP-based nanocomposite (BP-DcF@sPL) that, under NIR irradiation, induced localized hyperthermia, resulting in substantial tumor cell death accompanied by DAMP exposure. This process facilitated DC activation and significantly enhanced $CD8^+$ T cell infiltration into tumors. The critical role of T cells was confirmed through depletion experiments, wherein loss of $CD4^+$ or $CD8^+$ T cells abrogated the antitumor efficacy. In another study, BPQDs coated with

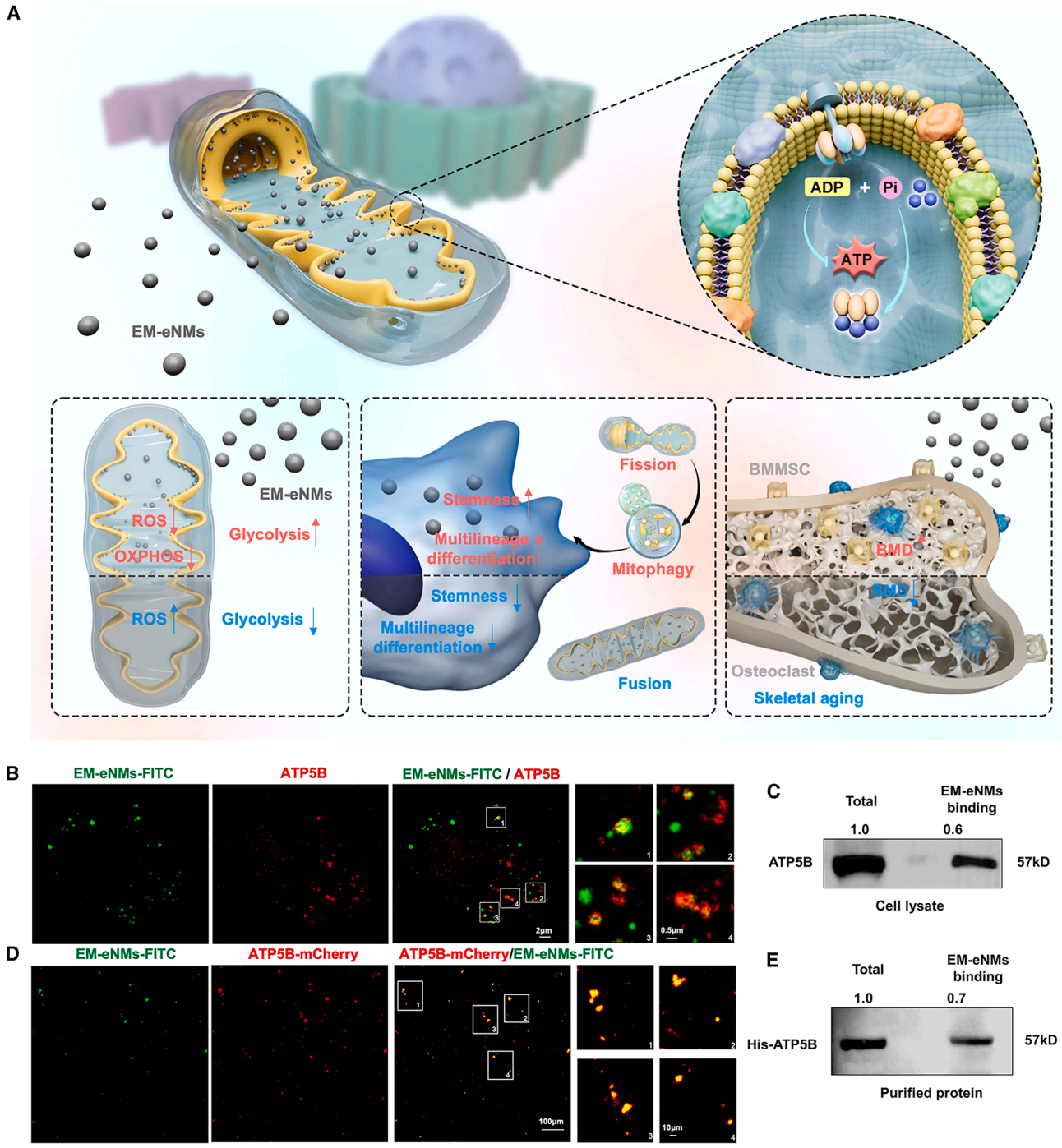

Figure 11. BP modulates cellular metabolism through direct interactions with biomolecules

(A) Schematic illustration showing that EM-eNMs rejuvenate aged BMMSCs and prevent skeletal aging by maintaining mitochondrial homeostasis.

(B) Immunofluorescent imaging of BMMSCs treated with EM-eNMs-FITC (green) for 24 h and stained for ATP5B (red).

(C) Immunoblotting of the EM-eNMs-protein complexes of BMMSCs incubated with EM-eNMs for 24 h.

(D) Immunofluorescent imaging of purified His-mCherry-ATP5B proteins treated with 1 μg mL^{-1} of EM-eNMs-FITC (green) for 4 h.

(E) Immunoblotting of the EM-eNMs-protein complexes of purified His-ATP5B proteins incubated with EM-eNMs for 4 h.[134] Copyright 2025, Springer Nature.

erythrocyte membranes (BPQD-RMNV) were demonstrated to augment PTT-mediated ICD. When used in combination with an anti-PD-1 antibody, this nanoplatform markedly suppressed the growth of both primary and metastatic tumors by synergistically enhancing antitumor immune responses (Figure 12A).[137]

In addition to the photothermal effect, BP nanomaterials also significantly enhance ICD through photodynamic pathways. Leveraging their strong optical absorption at specific wavelengths, BP nanomaterials generate substantial levels of ROS upon light irradiation, which serve as key mediators of ICD. Li et al.[139] constructed BP nanocapsules loaded with CpG oligodeoxynucleotides (BPNVs-CpG).[140] Under NIR irradiation, BP-generated ROS facilitated the release of CpG, which synergized with DAMPs to activate antigen-presenting cells and enhance cytokine production, thereby amplifying antitumor immunity. *In vitro* and *in vivo* experiments demonstrated that the PDT and immunotherapy triggered by BPNVs-CpG not only effectively cleared the primary tumor but also significantly inhibited tumor metastasis and growth. Further expanding this strategy, Ag^+-coupled BP vesicles (BP Ve-Ag^+) were developed for NIR-II PA imaging and combination therapy. The released Ag^+ ions promoted proinflammatory macrophage polarization and augmented ICD, thereby eliciting robust antitumor immunity.[141] Furthermore, BP-induced ICD has been shown to counteract tumor immune evasion mechanisms, highlighting its potential to overcome resistance in immunologically cold tumors. In a study by Xie et al.,[142] BP-based PTT combined with an anti-CD47 antibody was shown to disrupt the CD47-SIRPα "don't eat me" signal, thereby enhancing macrophage phagocytosis and promoting cross-presentation of tumor antigens. This combination strategy facilitated systemic T cell activation and effectively suppressed metastatic growth. Gas therapy combined with BP-mediated ICD represents another promising approach. Huang et al.[143] designed a nitric oxide (NO)-releasing BP system (NOPS@BP) that, under NIR light, released NO to act synergistically with BP-generated ROS. This dual stimulus induced endoplasmic reticulum stress and calreticulin exposure, strongly promoting DC maturation and CTL infiltration, while simultaneously inhibiting regulatory T cells and M2-type macrophage polarization.

BP directly activates immune cell function

Beyond regulating the immune microenvironment, BP nanomaterials exhibit specific interactions with various immune cell types at the cellular and molecular levels, including macrophages, DCs, and T cells, thereby triggering a cascade of intracellular signaling pathways. These direct interactions enable precise immunomodulatory effects, such as augmenting antigen presentation by DCs and regulating cytokine secretion in macrophages, highlighting the potential of BP-based strategies for targeted immunotherapy through specific immune cell activation.

Regarding anti-tumor immune activation, relevant studies have shown that BP can directly enhance the body's innate immune responses, addressing the significant barrier of immunosuppression in tumor immunity. For example, PEG-functionalized BP (BP-PEG) NSs were prepared to investigate their immunomodulatory effects in BC models. Bulk and single-cell RNA sequencing revealed that BP-PEG NSs were primarily absorbed by macrophages, leading to the release of inflammatory factors such as interleukin-1 alpha and C-X-C chemokine ligand 2 (CXCL2). These cytokines initiated a coordinated immune response through the CXCL2-C-X-C chemokine receptor 2 (CXCR2) signaling axis, recruiting and activating neutrophils that subsequently enhanced anti-tumor activity via intensified degranulation and ROS production.[144] Furthermore, BP nanomaterials directly enhanced NK cell function through concurrent activation of two signaling pathways: PIP5K1A-mediated metabolic reprogramming and TLR-triggered NF-κB signaling. This dual stimulation significantly augmented cytokine secretion and reinforced the cytotoxic capacity of NK cells against tumor targets (Figure 12B).[133]

While these immunostimulatory properties hold therapeutic potential, they also raise important safety considerations. The heightened immune response could lead to adverse effects, such as inflammation, autoimmune reactions, or even cytokine storms, which can be life-threatening. Mo et al.[7] revealed that protein corona-coated BP nanomaterials exhibit enhanced cellular uptake in macrophages, triggering substantial proinflammatory responses, including elevated TNF-α secretion and ROS overproduction. This immunotoxic potential underscores the need for surface engineering strategies to balance immune activation with safety profiles. Conversely, the inflammatory effects of BP nanomaterials can be leveraged for regenerative applications. In bone tissue engineering, BP was shown to stimulate macrophages to express IL-33, which not only potentiated early inflammatory signaling but also contributed to inflammation resolution and directly facilitated osteogenic differentiation of bone marrow MSCs (Figure 12C).[138]

These findings collectively establish BP nanomaterials as versatile immune cell activators, capable of directly engaging multiple immune cell types through specific receptor interactions and signaling pathways. The precise nature of these interactions offers exciting opportunities for developing targeted immunotherapies while simultaneously highlighting the importance of carefully evaluating immune-related toxicity profiles in the design of BP NMs.

CONCLUSION AND OUTLOOK

The past decade has witnessed intensive investigations into the fundamental properties and applications of BP, leading to substantial advances in catalysis, electronics, and biomedicine. Owing to its unique physicochemical characteristics and exceptional biocompatibility, BP has emerged as a promising nanomaterial for clinical translation. However, upon entry into the biological milieu, BP NMs often induce complex and multifaceted biological responses due to the intricacies of living systems. Therefore, a thorough understanding of the biological effects elicited by BP NMs and their correlation with intrinsic properties is critical.

This review first outlines the atomic structure and physicochemical characteristics of BP and then systematically summarizes the correlations between these fundamental properties and its diverse biological activities (Table 1). The biological responses elicited by BP nanomaterials are primarily attributed to their distinctive atomic configuration, semiconducting nature, high surface reactivity arising from non-bonded lone electron

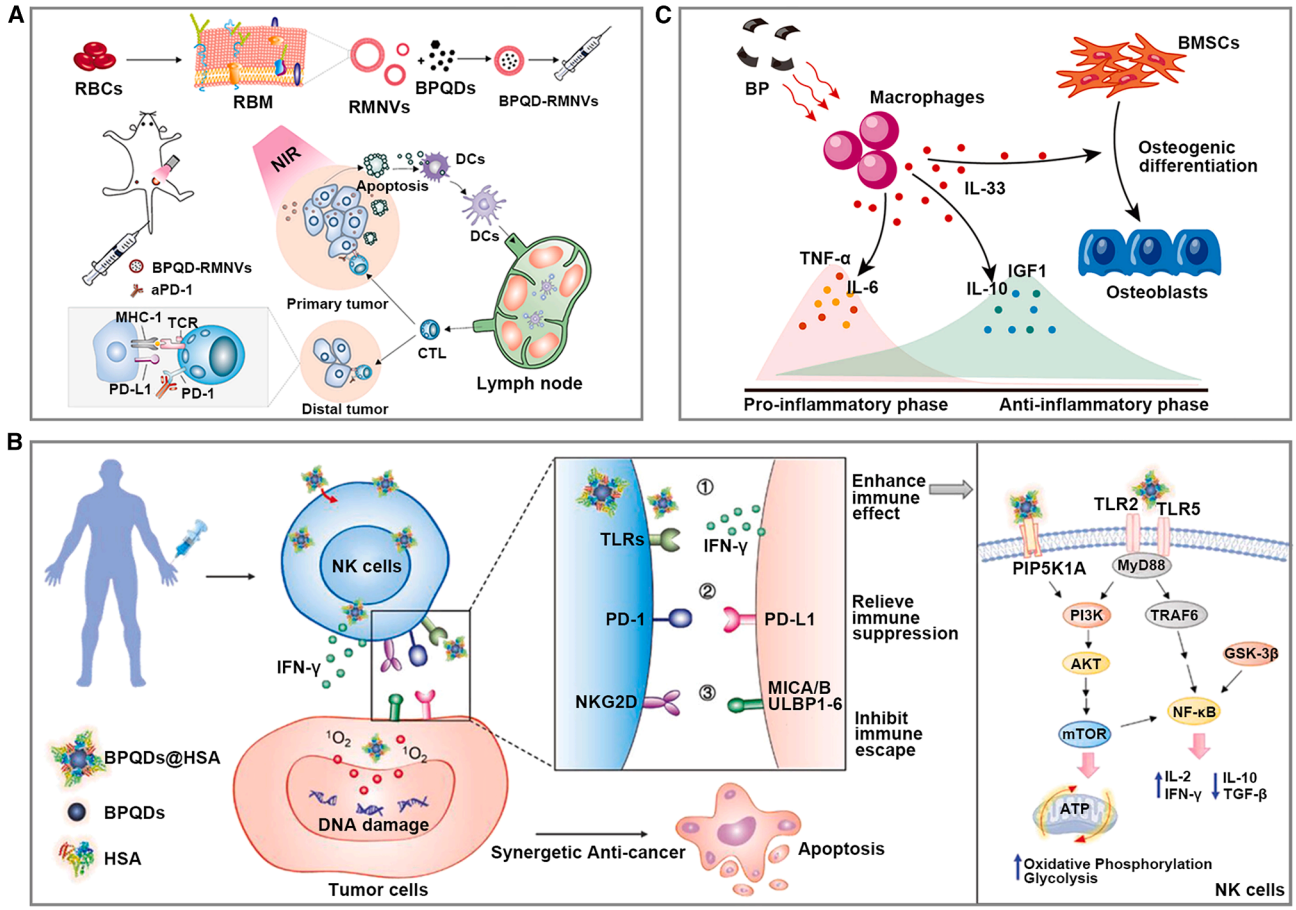

Figure 12. Immunomodulatory strategies based on BP NMs

(A) Schematic of photothermal cancer immunotherapy mediated by BPQD-RMNVs and aPD-1.[137] Copyright 2019, Elsevier.

(B) BPQDs@HSA enhances anticancer activity of NK cells.[133] Copyright 2023, Wiley-VCH.

(C) Schematic diagram of BP accelerates bone regeneration by stimulating the expression of IL-33 in macrophages.[138] Copyright 2024, Wiley-VCH.

pairs, and dynamic interactions at the bio-BP interface. These intrinsic properties enable BP NMs and their metabolites to exert a range of unique biological effects, including efficient photothermal conversion, redox modulation, and metabolic regulation. Such effects have been harnessed in diverse biomedical applications, notably in antioxidant therapy, PTT and PDT, tissue regeneration, and cancer treatment. Despite significant advances in understanding the relationship between BP's physicochemical properties and its biological effects, BP NMs still face substantial challenges in rational design and clinical translation.

First, the development of controllable, scalable, and biologically compatible synthesis strategies is urgently required to guarantee consistent production of high-quality BP NMs. Current methods predominantly rely on "top-down" approaches, which often involve organic solvents or harsh reaction conditions to minimize material degradation. These requirements, however, may introduce cytotoxic residues or complicate purification processes, thereby limiting clinical applicability. From a translational medicine perspective, scaling these laboratory-scale methods to industrial production while adhering to Good Manufacturing Practice (GMP) standards remains a significant challenge. Ensuring batch-to-batch consistency in size, stability, and purity is essential for regulatory approval, and ongoing technical innovations are continuously advancing toward this goal. Remarkably, unlike most other inorganic nanomaterials, BP is fully degradable, providing a potential advantage for future approval by pharmaceutical regulatory authorities. Nevertheless, although BP and its ultimate degradation products are generally considered non-toxic, their breakdown in complex redox environments may induce oxidative stress, compromise key biomolecules or organelle function, and elicit unpredictable biological effects. Therefore, systematic evaluation of BP and its intermediate degradation products—including *in vivo* safety, pharmacokinetics, metabolic pathways, and biodistribution—is essential to bridge the gap between preclinical studies and physiological responses, ensuring reliable clinical translation. Moreover, although current studies primarily focus on the preliminary therapeutic efficacy of BP NMs, their underlying mechanisms and structure-activity relationships remain insufficiently elucidated. A priority for future research is to decipher the biological effects of BP NMs at the cellular and molecular levels, elucidating their interactions with critical biomolecules and organelles

Table 1. Biological effects of BP NMs

	Materials	Cell type	Mechanism	Biological effect	Reference
Bioactivity driven by physical stimuli	BPQDs/GA/PLLA-PEG-PLLA	MCF-7, T47D, MCF-10A cell	thermal ablation and HSP90 inhibition	heat stress	Chen et al.[47]
	BP/hydrogel/emetine	Huh7 cell	thermal ablation and inhibiting SG formation	heat stress	Xie et al.[48]
	biomimetic BPQDs	4T1 cell	photothermal ablation and DC maturation promotion	heat stress and immune activation	Zhao et al.[56]
	BP NSs	–	upregulating fibrinogen and triggering PI3K/Akt and ERK1/2	oxidative stress	Mao et al.[65]
	BPQDs@NH	–	upregulating VEGF and bFGF, oxidative stress	heat stress and oxidative stress	Huang et al.[66]
	BP/Bi_2O_3	A375 cell	inducing apoptosis and cell-cycle arrest	oxidative stress	Oleinick et al.[79]
	RGD-Ir@BP	CNE-2, 6-10B, and NP69 cell	down-regulation prostaglandin E2	oxidative stress	Cai et al.[81]
	Au/BP@MS	MCF-7 cell	depletion of GSH and induction of oxidative stress	oxidative stress	Chen et al.[84]
	pDA-mBP@DAT	BMSCs	promotes osteogenesis and neovascularization, and activates Piezo1	tissue repair	Jia et al.[85]
	BPN-MnCO	SMCC-7721	inhibiting DNA damage repair and accelerating the ATM-GADD45-p53-cyclin B cell death signal	heat stress	Jin et al.[92]
	BPNs-PDA-PEG-PEITC-Mn/DOX	MCF-7 and MCF-7/ADR	decreasing mutant p53 level	heat stress and oxidative stress	Wu et al.[86]
Physiological modulation mediated by chemical reactivity	GM@CS-BP	NP cell	block the inflammatory cascade and reduce matrix metalloproteinase expression	regulation of oxygen metabolism	Li et al.[104]
	BP-Cu	SH-SY5Y	selective capture of Cu^{2+}	inflammatory microenvironment regulation	Chen et al.[108]
	BPNSs@PEG-S2P	RAW264.7	scavenge ROS and suppress pro-inflammatory cytokine production in lesional macrophages	inflammatory microenvironment regulation	He et al.[105]
	BP NSs	hBMSCs, QSG-7701, A549, MCF-7, and HeLa cell	inducing G2/M phase arrest, apoptosis and autophagy	cell cycle regulation	Zhou et al.[113]

(*Continued on next page*)

Table 1. *Continued*

	Materials	Cell type	Mechanism	Biological effect	Reference
	BP-PEG	Hela, and D551 cell	oxidative stress, arresting the cell cycle, inducing DNA damage and apoptosis	oxidative stress and cell cycle regulation	Kong et al.[114]
	BP NSs	A375, and HeLa cell	blocking glycolysis, autophagic flux	ion-interference	Yang et al.[118]
	CaP-mineralized BPs	MCF-7, Hela, A549, hBMSCs, and QSG-7701 cell	targeted mitochondrial damage	ion-interference	Pan et al.[117]
	BP@BMP2	BMSCs	recruitment of osteoblast precursor cells and promotion of biomineralizations	tissue repair	Cheng et al.[115]
	BPs@PLGA	BMSCs	upregulation of heat shock proteins, promotion of osteogenesis	tissue repair	Tong et al.[121]
	apt-bioinspired MVs	osteoblast	upregulation of heat shock proteins and alkaline phosphatase, and promotion of the biomineralization	tissue repair	Wang et al.[116]
	GelMA-BP@Mg	BMSCs	enhance early vascularization and neurogenesis	tissue repair	Xu et al.[125]
	BP NSs	BMSCs	promoting blood vessel formation and accelerating bone defect healing	tissue repair	Wang et al.[127]
Direct bio-interactions with biomolecules, organelles, and cells	BP NSs and BPQDs	H1299, L0-2, 293T, THP-1, SC cell	NF-κB pathway activation	immunotoxicology	Mo et al.[7]
	BP NSs	HeLa, A549, MDA-MB-231, U-2 OS, Hep G2 U-87 MG, HUVEC, RPE-1, and THP-1	induction of PLK1 aggregation, fragmentation of mitotic centrosomes	cell cycle regulation	Shao et al.[131]
	BP NSs	GL261 cell	binds to HSP90 protein and inhibits the PI3K-AKT signaling pathway	modulate the tumor immune microenvironment	Xiong et al.[132]
	BP NSs	PC12 cell	direct interaction with α-syn fibrils	treatment of neurological diseases	He et al.[129]
	EM-eNMs	BMMSCs	EM-eNMs directly bind to the ATP synthase and promote mitophagy	energy metabolism regulation	Chen et al.[134]
	BPQD-RMNV	4T1, 4T1-luc and $CD8^+$ T	increased infiltration and activity of $CD8^+$ T cells	heat stress and immune activation	Liang et al.[137]

(*Continued on next page*)

Table 1. *Continued*

	Materials	Cell type	Mechanism	Biological effect	Reference
	FKF-OVAp@BPs	B16-OVA	DC maturation promotion, cellular immune activation	heat stress and immune activation	Li et al.[145]
	BPQDs@HSA	HepG-2 and NK cell	activation of PI3K-Akt and mTOR pathways	immune activation	He et al.[133]
	BP-PEG	4T1 cell	promote neutrophil recruitment and activation	modulate the tumor immune microenvironment	Wang et al.[144]
	BP NSs	BMSCs	stimulating macrophages to express interleukin 33	immune activation	Qiu et al.[138]
	BPNVs-CPG	4T1 and MCF-7	ICD and induced anti-tumor immune response	immune activation	Zhang et al.[140]

BPQDs, black phosphorus quantum dots; BP NSs, black phosphorus nanosheets; GA, gambogic acid; PLLA-PEG-PLLA, poly(L-lactide)-poly(ethylene glycol)-poly(L-lactide) triblock copolymer; HSP, heat shock protein; PTT, Photothermal Therapy; SG, stress granule; DC, dendritic cell; MCF-7, human breast carcinoma cell line; DAT, decellularized adipose tissue; MT, matrine; PI3K, phosphoinositide 3-kinase;Akt, phosphorylation of protein kinase B; ERK1/2, extracellular signal-regulated kinase; PDT, Photodynamic Therapy; NH, encapsulated in hydrogel; MRSA, Methicillin-resistant Staphylococcus aureus; VEGF, vascular endothelial growth facto; bFGF, basic fibroblast growth factor ; BTA, 4-(6-methyl-1,3-benzothiazol-2-yl) phenylamine; $^1O_2$, singlet oxygen; Aβ, amyloid-β; HA, hyaluronate; DAH, diaminohexane; RGD, Arg-Gly-Asp; ATM, ataxia telangiectasia mutated; GADD45, growth arrest and DNA damage-inducible 45; HepG2, liver cancer cells; PDA, polydopamine; PEG, polyethylene glycol; PEITC, phenethyl isothiocyanate; DOX, doxorubicin; ND, neurodegenerative disorder; CaP, calcium phosphate; PLGA, poly(lactic-co-glycolic acid); GelMA, gelatin methacryloyl; NF-κB, nuclear factor kappa-light-chain-enhancer of activated B-cells; PLK1, Polo-like kinase 1; RM, Erythrocyte membrane; NV, nanovesicle; FKF, phenylalanine-lysine-phenylalanine; OVAp, antigen peptide; HAS, human serum albumin; NK, Natural killer; mTOR, mammalian target of rapamycin; ICD, immunogenic cell death; BMSCs, bone marrow mesenchymal stem cells.

to guide the rational and targeted design of BP-based therapeutics. Finally, the highly reactive surface of BP offers broad opportunities for structural tuning and functionalization. Rational surface modification can enhance stability under physiological conditions and modulate interactions with biological systems. However, while functionalization can improve material performance, it also increases the complexity of safety and toxicological evaluation. Future strategies must carefully balance therapeutic efficacy and biosafety and systematically assess the biocompatibility and systemic toxicity of functionalized BP NMs.

In conclusion, with ongoing research shedding light on BP's exceptional characteristics and underlying biological mechanisms, it is anticipated that BP MNs are poised to unlock transformative opportunities across a broad spectrum of cutting-edge biomedical applications. Addressing key translational considerations—from scalable, GMP-compliant manufacturing to robust preclinical-to-clinical extrapolation—will be accelerated through interdisciplinary collaboration among material scientists, clinicians, and regulatory experts, paving the way for BP-based NMs to successfully transition from the laboratory bench to clinical practice.

ACKNOWLEDGMENTS

Y.F., L.C., and J.Z. contributed equally to this paper. The authors are grateful for the support received from the National Key Research and Development Program of China (2022YFB3205602), the National Natural Science Foundation of China (52372174, 32401198, 82230030, T2125003), the Beijing Natural Science Foundation (JL23002), and the Beijing Nova Programme Interdisciplinary Cooperation Project (No.20250484970).

AUTHOR CONTRIBUTIONS

Y.F.: investigation, writing - original draft. L.C.: investigation, writing - original draft. J.Z.: investigation, writing - original draft. C.L.: writing - review & editing. L.L.: formal analysis. R.L.: writing original draft, formal analysis. S.X.: formal analysis. Z.L.: conceptualization, writing review & editing. Y.L.: conceptualization, writing - review & editing. D.L.: conceptualization, writing - review & editing.

DECLARATION OF INTERESTS

The authors declare no competing interests.

REFERENCES

1. Dai, J., and Zeng, X.C. (2014). Bilayer phosphorene: effect of stacking order on bandgap and its potential applications in thin-film solar cells. J. Phys. Chem. Lett. *5*, 1289–1293. https://doi.org/10.1021/jz500409m.
2. Jiang, J.W., and Park, H.S. (2014). Negative poisson's ratio in single-layer black phosphorus. Nat. Commun. *5*, 4727. https://doi.org/10.1038/ncomms5727.
3. Qiao, J., Kong, X., Hu, Z.X., Yang, F., and Ji, W. (2014). High-mobility transport anisotropy and linear dichroism in few-layer black phosphorus. Nat. Commun. *5*, 4475. https://doi.org/10.1038/ncomms5475.
4. Qiu, M., Ren, W.X., Jeong, T., Won, M., Park, G.Y., Sang, D.K., Liu, L.P., Zhang, H., and Kim, J.S. (2018). Omnipotent phosphorene: a next-generation, two-dimensional nanoplatform for multidisciplinary biomedical applications. Chem. Soc. Rev. *47*, 5588–5601. https://doi.org/10.1039/c8cs00342d.
5. Huang, K., Wu, J., and Gu, Z. (2019). Black phosphorus hydrogel scaffolds enhance bone regeneration via a sustained supply of

calcium-free phosphorus. ACS Appl. Mater. Interfaces *11*, 2908–2916. https://doi.org/10.1021/acsami.8b21179.

6. Qu, G., Xia, T., Zhou, W., Zhang, X., Zhang, H., Hu, L., Shi, J., Yu, X.F., and Jiang, G. (2020). Property-activity relationship of black phosphorus at the nano-bio interface: from molecules to organisms. Chem. Rev. *120*, 2288–2346. https://doi.org/10.1021/acs.chemrev.9b00445.
7. Mo, J., Xie, Q., Wei, W., and Zhao, J. (2018). Revealing the immune perturbation of black phosphorus nanomaterials to macrophages by understanding the protein corona. Nat. Commun. *9*, 2480. https://doi.org/10.1038/s41467-018-04873-7.
8. Bridgman, P.W. (1914). Two new modifications of phosphorus. J. Am. Chem. Soc. *36*, 1344–1363. https://doi.org/10.1021/ja02184a002.
9. Li, L., Yu, Y., Ye, G.J., Ge, Q., Ou, X., Wu, H., Feng, D., Chen, X.H., and Zhang, Y. (2014). Black phosphorus field-effect transistors. Nat. Nanotechnol. *9*, 372–377. https://doi.org/10.1038/Nnano.2014.35.
10. Ziletti, A., Carvalho, A., Campbell, D.K., Coker, D.F., and Castro Neto, A.H. (2015). Oxygen defects in phosphorene. Phys. Rev. Lett. *114*, 046801. https://doi.org/10.1103/PhysRevLett.114.046801.
11. Tao, W., Kong, N., Ji, X., Zhang, Y., Sharma, A., Ouyang, J., Qi, B., Wang, J., Xie, N., Kang, C., et al. (2019). Emerging two-dimensional monoelemental materials (Xenes) for biomedical applications. Chem. Soc. Rev. *48*, 2891–2912. https://doi.org/10.1039/c8cs00823j.
12. Liu, H., Neal, A.T., Zhu, Z., Luo, Z., Xu, X., Tománek, D., and Ye, P.D. (2014). Phosphorene: an unexplored 2D semiconductor with a high hole mobility. ACS Nano *8*, 4033–4041. https://doi.org/10.1021/nn501226z.
13. Shulenburger, L., Baczewski, A.D., Zhu, Z., Guan, J., and Tománek, D. (2015). The nature of the inter layer interaction in bulk and few-layer phosphorus. Nano Lett. *15*, 8170–8175. https://doi.org/10.1021/acs.nanolett.5b03615.
14. Guo, Z., Zhang, H., Lu, S., Wang, Z., Tang, S., Shao, J., Sun, Z., Xie, H., Wang, H., Yu, X.F., and Chu, P.K. (2015). From black phosphorus to phosphorene: basic solvent exfoliation, evolution of raman scattering, and applications to ultrafast photonics. Adv. Funct. Mater. *25*, 6996–7002. https://doi.org/10.1002/adfm.201502902.
15. Tan, C., Cao, X., Wu, X.J., He, Q., Yang, J., Zhang, X., Chen, J., Zhao, W., Han, S., Nam, G.-H., et al. (2017). Recent advances in ultrathin two-dimensional nanomaterials. Chem. Rev. *117*, 6225–6331. https://doi.org/10.1021/acs.chemrev.6b00558.
16. Sun, Z., Xie, H., Tang, S., Yu, X.F., Guo, Z., Shao, J., Zhang, H., Huang, H., Wang, H., and Chu, P.K. (2015). Ultrasmall black phosphorus quantum dots: synthesis and use as photothermal agents. Angew. Chem. Int. Ed. *54*, 11526–11530. https://doi.org/10.1002/anie.201506154.
17. Wang, H., Yang, X., Shao, W., Chen, S., Xie, J., Zhang, X., Wang, J., and Xie, Y. (2015). Ultrathin black phosphorus nanosheets for efficient singlet oxygen generation. J. Am. Chem. Soc. *137*, 11376–11382. https://doi.org/10.1021/jacs.5b06025.
18. Hou, J., Wang, H., Ge, Z., Zuo, T., Chen, Q., Liu, X., Mou, S., Fan, C., Xie, Y., and Wang, L. (2020). Treating acute kidney injury with antioxidative black phosphorus nanosheets. Nano Lett. *20*, 1447–1454. https://doi.org/10.1021/acs.nanolett.9b05218.
19. Zhou, Q., Chen, Q., Tong, Y., and Wang, J. (2016). Light-induced ambient degradation of few-layer black phosphorus: mechanism and protection. Angew. Chem. Int. Ed. *55*, 11437–11441. https://doi.org/10.1002/anie.201605168.
20. Asahina, H., and Morita, A. (1984). Band-structure and optical-properties of black phosphorus. J. Phys. C Solid State Phys. *17*, 1839–1852. https://doi.org/10.1088/0022-3719/17/11/006.
21. Rodin, A.S., Carvalho, A., and Castro Neto, A.H. (2014). Strain-induced gap modification in black phosphorus. Phys. Rev. Lett. *112*, 176801. https://doi.org/10.1103/PhysRevLett.112.176801.
22. Kang, Y., Zhang, H., Chen, L., Dong, J., Yao, B., Yuan, X., Qin, D., Yaremenko, A.V., Liu, C., Feng, C., et al. (2022). The marriage of Xenes and hydrogels: Fundamentals, applications, and outlook. Innovation *3*, 100327. https://doi.org/10.1016/j.xinn.2022.100327.
23. Ji, X., Kang, Y., Fan, T., Xiong, Q., Zhang, S., Tao, W., and Zhang, H. (2020). An antimonene/Cp*Rh(phen)Cl/black phosphorus hybrid nanosheet-based Z-scheme artificial photosynthesis for enhanced photo/bio-catalytic CO_2 reduction. J. Mater. Chem. A *8*, 323–333. https://doi.org/10.1039/c9ta11167k.
24. Hessel, C.M., Pattani, V.P., Rasch, M., Panthani, M.G., Koo, B., Tunnell, J.W., and Korgel, B.A. (2011). Copper selenide nanocrystals for photothermal therapy. Nano Lett. *11*, 2560–2566. https://doi.org/10.1021/nl201400z.
25. Sun, C., Wen, L., Zeng, J., Wang, Y., Sun, Q., Deng, L., Zhao, C., and Li, Z. (2016). One-pot solventless preparation of PEGylated black phosphorus nanoparticles for photoacoustic imaging and photothermal therapy of cancer. Biomaterials *91*, 81–89. https://doi.org/10.1016/j.biomaterials.2016.03.022.
26. Favron, A., Gaufrès, E., Fossard, F., Phaneuf-L'Heureux, A.L., Tang, N.Y.W., Lévesque, P.L., Loiseau, A., Leonelli, R., Francoeur, S., and Martel, R. (2015). Photooxidation and quantum confinement effects in exfoliated black phosphorus. Nat. Mater. *14*, 826–832. https://doi.org/10.1038/Nmat4299.
27. Yau, S.L., Moffat, T.P., Bard, A.J., Zhang, Z., and Lerner, M.M. (1992). Stm of the (010) surface of orthorhombic phosphorus. Chem. Phys. Lett. *198*, 383–388. https://doi.org/10.1016/0009-2614(92)85069-M.
28. Ryder, C.R., Wood, J.D., Wells, S.A., Yang, Y., Jariwala, D., Marks, T.J., Schatz, G.C., and Hersam, M.C. (2016). Covalent functionalization and passivation of exfoliated black phosphorus via aryl diazonium chemistry. Nat. Chem. *8*, 597–602. https://doi.org/10.1038/Nchem.2505.
29. Yu, S., Du, Y., Niu, X., Li, G., Zhu, D., Yu, Q., Zou, G., and Ju, H. (2022). Arginine-modified black phosphorus quantum dots with dual excited states for enhanced electrochemiluminescence in bioanalysis. Nat. Commun. *13*, 7302. https://doi.org/10.1038/s41467-022-35015-9.
30. Guo, Z., Chen, S., Wang, Z., Yang, Z., Liu, F., Xu, Y., Wang, J., Yi, Y., Zhang, H., Liao, L., et al. (2017). Metal-ion-modified black phosphorus with enhanced stability and transistor performance. Adv. Mater. *29*, 1703811. https://doi.org/10.1002/adma.201703811.
31. Tao, W., Zhu, X., Yu, X., Zeng, X., Xiao, Q., Zhang, X., Ji, X., Wang, X., Shi, J., Zhang, H., and Mei, L. (2017). Black phosphorus nanosheets as a robust delivery platform for cancer theranostics. Adv. Mater. *29*, 1603276. https://doi.org/10.1002/adma.201603276.
32. Shao, J., Xie, H., Huang, H., Li, Z., Sun, Z., Xu, Y., Xiao, Q., Yu, X.F., Zhao, Y., Zhang, H., et al. (2016). Biodegradable black phosphorus-based nanospheres for in vivo photothermal cancer therapy. Nat. Commun. *7*, 12967. https://doi.org/10.1038/ncomms12967.
33. Liu, J., Yi, K., Zhang, Q., Xu, H., Zhang, X., He, D., Wang, F., and Xiao, X. (2021). Strong penetration-induced effective photothermal therapy by exosome-mediated black phosphorus quantum dots. Small *17*, 2104585. https://doi.org/10.1002/smll.202104585.
34. Lee, H.U., Park, S.Y., Lee, S.C., Choi, S., Seo, S., Kim, H., Won, J., Choi, K., Kang, K.S., Park, H.G., et al. (2016). Black phosphorus (BP) nanodots for potential biomedical applications. Small *12*, 214–219. https://doi.org/10.1002/smll.201502756.
35. Song, S.J., Raja, I.S., Lee, Y.B., Kang, M.S., Seo, H.J., Lee, H.U., and Han, D.W. (2019). Comparison of cytotoxicity of black phosphorus nanosheets in different types of fibroblasts. Biomater. Res. *23*, 23. https://doi.org/10.1186/s40824-019-0174-x.
36. Chen, J., Huan, W., Mao, L., Huang, M., Wu, Y., Zhuang, S., and Cui, S. (2023). Impaired barrier integrity of endothelial cells induced by PEGylated black phosphorus nanosheets. Sci. Total Environ. *861*, 160645. https://doi.org/10.1016/j.scitotenv.2022.160645.
37. Zhang, X., Zhang, Z., Zhang, S., Li, D., Ma, W., Ma, C., Wu, F., Zhao, Q., Yan, Q., and Xing, B. (2017). Size effect on the cytotoxicity of layered

black phosphorus and underlying mechanisms. Small *13*, 1701210. https://doi.org/10.1002/smll.201701210.

38. Cheng, L., Cai, Z., Zhao, J., Wang, F., Lu, M., Deng, L., and Cui, W. (2020). Black phosphorus-based 2D materials for bone therapy. Bioact. Mater. *5*, 1026–1043. https://doi.org/10.1016/j.bioactmat.2020.06.007.

39. Ouyang, J., Feng, C., Zhang, X., Kong, N., and Tao, W. (2021). Black phosphorus in biological applications: Evolutionary journey from monoelemental materials to composite materials. Acc. Mater. Res. *2*, 489–500. https://doi.org/10.1021/accountsmr.1c00039.

40. Qin, H., Chen, J., Li, Y., Gao, L., Wang, J., Qu, G., Yang, M., Zhou, X., and Sun, Z. (2021). Inflammatory response induced by black phosphorus nanosheets in mice and macrophages. Sci. Total Environ. *782*, 146860. https://doi.org/10.1016/j.scitotenv.2021.146860.

41. Wang, Y., Li, M., Wang, S., Ma, J., Liu, Y., Guo, H., Gao, J., Yao, L., He, B., Hu, L., et al. (2022). Deciphering the effects of 2D black phosphorus on disrupted hematopoiesis and pulmonary immune homeostasis using a developed flow cytometry method. Environ. Sci. Technol. *56*, 15869–15881. https://doi.org/10.1021/acs.est.2c03675.

42. Wang, J., Hou, J., Lu, H., Bai, S., Chen, Y., Yang, W., Wang, S., Li, G., Wei, Y., Wang, X., and Xie, W. (2025). Engineering programmable nanobiomaterials (PNBMs) for cancer nanotherapy. MedMat *2*, 1–16. https://doi.org/10.1097/mm9.0000000000000011.

43. Zhao, F., Zhao, Z., Gao, H., Zhang, Y., Qi, J., Yu, H., Wang, C., Xu, J., Zubair Yousaf, M., Che, S., and Yu, J. (2024). Cuproptosis: an emerging domain for copper-based nanomaterials mediated cancer therapy. MedMat *1*, 74–94. https://doi.org/10.1097/mm9.0000000000000010.

44. Ouyang, J., Ji, X., Zhang, X., Feng, C., Tang, Z., Kong, N., Xie, A., Wang, J., Sui, X., Deng, L., et al. (2020). In situ sprayed NIR-responsive, analgesic black phosphorus-based gel for diabetic ulcer treatment. Proc. Natl. Acad. Sci. USA *117*, 28667–28677. https://doi.org/10.1073/pnas.2016268117.

45. Wang, D., Ge, C., Liang, W., Yang, Q., Liu, Q., Ma, W., Shi, L., Wu, H., Zhang, Y., Wu, Z., et al. (2020). In vivo enrichment and elimination of circulating tumor cells by using a black phosphorus and antibody functionalized intravenous catheter. Adv. Sci. *7*, 2000940. https://doi.org/10.1002/advs.202000940.

46. Melamed, J.R., Edelstein, R.S., and Day, E.S. (2015). Elucidating the fundamental mechanisms of cell death triggered by photothermal therapy. ACS Nano *9*, 6–11. https://doi.org/10.1021/acsnano.5b00021.

47. Chen, B.Q., Kankala, R.K., Zhang, Y., Xiang, S.T., Tang, H.X., Wang, Q., Yang, D.Y., Wang, S.B., Zhang, Y.S., Liu, G., and Chen, A.Z. (2020). Gambogic acid augments black phosphorus quantum dots (BPQDs)-based synergistic chemo-photothermal therapy through downregulating heat shock protein expression. Chem. Eng. J. *390*, 124312. https://doi.org/10.1016/j.cej.2020.124312.

48. Xie, J., Fan, T., Kim, J.H., Xu, Y., Wang, Y., Liang, W., Qiao, L., Wu, Z., Liu, Q., Hu, W., et al. (2020). Emetine-loaded black phosphorus hydrogel sensitizes tumor to photothermal therapy through inhibition of stress granule formation. Adv. Funct. Mater. *30*, 2003891. https://doi.org/10.1002/adfm.202003891.

49. Deng, X., Liu, H., Xu, Y., Chan, L., Xie, J., Xiong, Z., Tang, Z., Yang, F., and Chen, T. (2021). Designing highly stable ferrous selenide-black phosphorus nanosheets heteronanostructure via P-Se bond for MRI-guided photothermal therapy. J. Nanobiotechnol. *19*, 201–220. https://doi.org/10.1186/s12951-021-00905-5.

50. Zhao, Y., Wang, H., Huang, H., Xiao, Q., Xu, Y., Guo, Z., Xie, H., Shao, J., Sun, Z., Han, W., et al. (2016). Surface coordination of black phosphorus for robust air and water stability. Angew. Chem. Int. Ed. *55*, 5003–5007. https://doi.org/10.1002/anie.201512038.

51. Li, Z., Wei, L., Gao, M.Y., and Lei, H. (2005). One-pot reaction to synthesize biocompatible magnetite nanoparticles. Adv. Mater. *17*, 1001–1005. https://doi.org/10.1002/adma.200401545.

52. Deng, L., Xu, Y., Sun, C., Yun, B., Sun, Q., Zhao, C., and Li, Z. (2018). Functionalization of small black phosphorus nanoparticles for targeted imaging and photothermal therapy of cancer. Sci. Bull. *63*, 917–924. https://doi.org/10.1016/j.scib.2018.05.022.

53. Li, Z., Xu, H., Shao, J., Jiang, C., Zhang, F., Lin, J., Zhang, H., Li, J., and Huang, P. (2019). Polydopamine-functionalized black phosphorus quantum dots for cancer theranostics. Appl. Mater. Today *15*, 297–304. https://doi.org/10.1016/j.apmt.2019.02.002.

54. Chen, L., Hong, W., Ren, W., Xu, T., Qian, Z., and He, Z. (2021). Recent progress in targeted delivery vectors based on biomimetic nanoparticles. Signal Transduct. Target. Ther. *6*, 225. https://doi.org/10.1038/s41392-021-00631-2.

55. Cao, Y., Wu, T., Zhang, K., Meng, X., Dai, W., Wang, D., Dong, H., and Zhang, X. (2019). Engineered exosome-mediated near-infrared-II region V_2C quantum dot delivery for nucleus-target low-temperature photothermal therapy. ACS Nano *13*, 1499–1510. https://doi.org/10.1021/acsnano.8b07224.

56. Zhao, P., Xu, Y., Ji, W., Zhou, S., Li, L., Qiu, L., Qian, Z., Wang, X., and Zhang, H. (2021). Biomimetic black phosphorus quantum dots-based photothermal therapy combined with anti-PD-L1 treatment inhibits recurrence and metastasis in triple-negative breast cancer. J. Nanobiotechnol. *19*, 181. https://doi.org/10.1186/s12951-021-00932-2.

57. Luo, M., Zhou, Y., Gao, N., Cheng, W., Wang, X., Cao, J., Zeng, X., Liu, G., and Mei, L. (2020). Mesenchymal stem cells transporting black phosphorus-based biocompatible nanospheres: active trojan horse for enhanced photothermal cancer therapy. Chem. Eng. J. *385*, 123942. https://doi.org/10.1016/j.cej.2019.123942.

58. Gao, Z., Zhang, Y., Liu, Q., and Ding, D. (2024). Mechanism and design of organic afterglow luminescent probes for cancer theranostics. MedMat *1*, 27–39. https://doi.org/10.1097/mm9.0000000000000003.

59. Schweitzer, C., and Schmidt, R. (2003). Physical mechanisms of generation and deactivation of singlet oxygen. Chem. Rev. *103*, 1685–1757. https://doi.org/10.1021/cr010371d.

60. Moan, J. (1990). On the diffusion length of singlet oxygen in cells and tissues. J. Photochem. Photobiol., B *6*, 343–344. https://doi.org/10.1016/1011-1344(90)85104-5.

61. Guo, T., Wu, Y., Lin, Y., Xu, X., Lian, H., Huang, G., Liu, J.Z., Wu, X., and Yang, H.H. (2018). Black phosphorus quantum dots with renal clearance property for efficient photodynamic therapy. Small *14*, 1702815. https://doi.org/10.1002/smll.201702815.

62. Liang, M., Zhang, M., Yu, S., Wu, Q., Ma, K., Chen, Y., Liu, X., Li, C., and Wang, F. (2020). Silver-laden black phosphorus nanosheets for an efficient in vivo antimicrobial application. Small *16*, 1905938. https://doi.org/10.1002/smll.201905938.

63. Li, M., Liu, X., Tan, L., Cui, Z., Yang, X., Li, Z., Zheng, Y., Yeung, K.W.K., Chu, P.K., and Wu, S. (2018). Noninvasive rapid bacteria-killing and acceleration of wound healing through photothermal/photodynamic/copper ion synergistic action of a hybrid hydrogel. Biomater. Sci. *6*, 2110–2121. https://doi.org/10.1039/c8bm00499d.

64. Zhang, D., Liu, H.M., Shu, X., Feng, J., Yang, P., Dong, P., Xie, X., and Shi, Q. (2020). Nanocopper-loaded black phosphorus nanocomposites for efficient synergistic antibacterial application. J. Hazard. Mater. *393*, 122317. https://doi.org/10.1016/j.jhazmat.2020.122317.

65. Mao, C., Xiang, Y., Liu, X., Cui, Z., Yang, X., Li, Z., Zhu, S., Zheng, Y., Yeung, K.W.K., and Wu, S. (2018). Repeatable photodynamic therapy with triggered signaling pathways of fibroblast cell proliferation and differentiation to promote bacteria-accompanied wound healing. ACS Nano *12*, 1747–1759. https://doi.org/10.1021/acsnano.7b08500.

66. Huang, S., Xu, S., Hu, Y., Zhao, X., Chang, L., Chen, Z., and Mei, X. (2022). Preparation of NIR-responsive, ROS-generating and antibacterial black phosphorus quantum dots for promoting the MRSA-infected wound healing in diabetic rats. Acta Biomater. *137*, 199–217. https://doi.org/10.1016/j.actbio.2021.10.008.

67. Qi, F., Ji, P., Chen, Z., Wang, L., Yao, H., Huo, M., and Shi, J. (2021). Photosynthetic cyanobacteria-hybridized black phosphorus nanosheets for enhanced tumor photodynamic therapy. Small *17*, 2102113. https://doi.org/10.1002/smll.202102113.

68. Huang, H., He, L., Zhou, W., Qu, G., Wang, J., Yang, N., Gao, J., Chen, T., Chu, P.K., and Yu, X.F. (2018). Stable black phosphorus/Bi_2O_3 heterostructures for synergistic cancer radiotherapy. Biomaterials *171*, 12–22. https://doi.org/10.1016/j.biomaterials.2018.04.022.

69. Dai, Y., Xu, C., Sun, X., and Chen, X. (2017). Nanoparticle design strategies for enhanced anticancer therapy by exploiting the tumour microenvironment. Chem. Soc. Rev. *46*, 3830–3852. https://doi.org/10.1039/c6cs00592f.

70. Hu, X., Lu, Y., Shi, X., Yao, T., Dong, C., and Shi, S. (2019). Integrating in situ formation of nanozymes with mesoporous polydopamine for combined chemo, photothermal and hypoxia-overcoming photodynamic therapy. Chem. Commun. *55*, 14785–14788. https://doi.org/10.1039/c9cc07125c.

71. Liu, J., Du, P., Liu, T., Córdova Wong, B.J., Wang, W., Ju, H., and Lei, J. (2019). A black phosphorus/manganese dioxide nanoplatform: oxygen self-supply monitoring, photodynamic therapy enhancement and feedback. Biomaterials *192*, 179–188. https://doi.org/10.1016/j.biomaterials.2018.10.018.

72. Wu, Q., Chen, G., Gong, K., Wang, J., Ge, X., Liu, X., Guo, S., and Wang, F. (2019). MnO_2-Laden black phosphorus for MRI-guided synergistic PDT, PTT, and chemotherapy. Matter *1*, 496–512. https://doi.org/10.1016/j.matt.2019.03.007.

73. Liu, J., Du, P., Mao, H., Zhang, L., Ju, H., and Lei, J. (2018). Dual-triggered oxygen self-supply black phosphorus nanosystem for enhanced photodynamic therapy. Biomaterials *172*, 83–91. https://doi.org/10.1016/j.biomaterials.2018.04.051.

74. Liu, J., Liu, T., Du, P., Zhang, L., and Lei, J. (2019). Metal-organic framework (MOF) hybrid as a tandem catalyst for enhanced therapy against hypoxic tumor cells. Angew. Chem. Int. Ed. *58*, 7808–7812. https://doi.org/10.1002/anie.201903475.

75. Bizic, M., Klintzsch, T., Ionescu, D., Hindiyeh, M.Y., Gunthel, M., Muro-Pastor, A.M., Eckert, W., Urich, T., Keppler, F., and Grossart, H.P. (2020). Aquatic and terrestrial cyanobacteria produce methane. Sci. Adv. *6*, eaax5343. https://doi.org/10.1126/sciadv.aax5343.

76. Fan, W., Huang, P., and Chen, X. (2016). Overcoming the achilles' heel of photodynamic therapy. Chem. Soc. Rev. *45*, 6488–6519. https://doi.org/10.1039/c6cs00616g.

77. Tan, L., Li, J., Liu, X., Cui, Z., Yang, X., Yeung, K.W.K., Pan, H., Zheng, Y., Wang, X., and Wu, S. (2018). In situ disinfection through photoinspired radical oxygen species storage and thermal-triggered release from black phosphorous with strengthened chemical stability. Small *14*, 1703197. https://doi.org/10.1002/smll.201703197.

78. Ma, L., Zou, X., Bui, B., Chen, W., Song, K.H., and Solberg, T. (2014). X-ray excited ZnS:Cu,Co afterglow nanoparticles for photodynamic activation. Appl. Phys. Lett. *105*, 013702. https://doi.org/10.1063/1.4890105.

79. Oleinick, N.L., Morris, R.L., and Belichenko, I. (2002). The role of apoptosis in response to photodynamic therapy: what, where, why, and how. Photochem. Photobiol. Sci. *1*, 1–21. https://doi.org/10.1039/b108586g.

80. Chan, L., Chen, X., Gao, P., Xie, J., Zhang, Z., Zhao, J., and Chen, T. (2021). Coordination-driven enhancement of radiosensitization by black phosphorus via regulating tumor metabolism. ACS Nano *15*, 3047–3060. https://doi.org/10.1021/acsnano.0c09454.

81. Cai, X., Mao, L., Yang, S., Han, K., and Zhang, J. (2018). Ultrafast charge separation for full solar spectrum-activated photocatalytic H_2 generation in a black phosphorus-Au-CdS heterostructure. ACS Energy Lett. *3*, 932–939. https://doi.org/10.1021/acsenergylett.8b00126.

82. Li, Z., Zhang, T., Fan, F., Gao, F., Ji, H., and Yang, L. (2020). Piezoelectric materials as donodynamic densitizers to dafely sblate tumors: a case study using black phosphorus. J. Phys. Chem. Lett. *11*, 1228–1238. https://doi.org/10.1021/acs.jpclett.9b03769.

83. Liu, Y., Li, Z., Fan, F., Zhu, X., Jia, L., Chen, M., Du, P., Yang, L., and Yang, S. (2021). Boosting antitumor sonodynamic therapy efficacy of black phosphorus via covalent functionalization. Adv. Sci. *8*, 2102422. https://doi.org/10.1002/advs.202102422.

84. Chen, T., Zeng, W., Tie, C., Yu, M., Hao, H., Deng, Y., Li, Q., Zheng, H., Wu, M., and Mei, L. (2022). Engineered gold/black phosphorus nanoplatforms with remodeling tumor microenvironment for sonoactivated catalytic tumor theranostics. Bioact. Mater. *10*, 515–525. https://doi.org/10.1016/j.bioactmat.2021.09.016.

85. Jia, W., Wang, T., Chen, F., Liu, Z., Hou, X., Cao, W., Zhao, X., Lu, B., Hu, Y., Dong, Y., et al. (2025). Low-intensity pulsed ultrasound responsive scaffold promotes intramembranous and endochondral ossification via ultrasonic, thermal, and electrical stimulation. ACS Nano *19*, 4422–4439. https://doi.org/10.1021/acsnano.4c13357.

86. Wu, F., Zhang, M., Chu, X., Zhang, Q., Su, Y., Sun, B., Lu, T., Zhou, N., Zhang, J., Wang, J., and Yi, X. (2019). Black phosphorus nanosheets-based nanocarriers for enhancing chemotherapy drug sensitiveness via depleting mutant p53 and resistant cancer multimodal therapy. Chem. Eng. J. *370*, 387–399. https://doi.org/10.1016/j.cej.2019.03.228.

87. Hu, K., Xie, L., Zhang, Y., Hanyu, M., Yang, Z., Nagatsu, K., Suzuki, H., Ouyang, J., Ji, X., Wei, J., et al. (2020). Marriage of black phosphorus and Cu^{2+} as effective photothermal agents for PET-guided combination cancer therapy. Nat. Commun. *11*, 2778. https://doi.org/10.1038/s41467-020-16513-0.

88. Zhang, Q., Wang, W., Zhang, M., Wu, F., Zheng, T., Sheng, B., Liu, Y., Shen, J., Zhou, N., and Sun, Y. (2020). A theranostic nanocomposite with integrated black phosphorus nanosheet, Fe_3O_4@MnO_2-doped upconversion nanoparticles and chlorin for simultaneous multimodal imaging, highly efficient photodynamic and photothermal therapy. Chem. Eng. J. *391*, 123525. https://doi.org/10.1016/j.cej.2019.123525.

89. Chen, Q., Wang, C., Cheng, L., He, W., Cheng, Z., and Liu, Z. (2014). Protein modified upconversion nanoparticles for imaging-guided combined photothermal and photodynamic therapy. Biomaterials *35*, 2915–2923. https://doi.org/10.1016/j.biomaterials.2013.12.046.

90. Liu, G., Tsai, H.I., Zeng, X., Qi, J., Luo, M., Wang, X., Mei, L., and Deng, W. (2019). Black phosphorus nanosheets-based stable drug delivery system via drug-self-stabilization for combined photothermal and chemo cancer therapy. Chem. Eng. J. *375*, 121917. https://doi.org/10.1016/j.cej.2019.121917.

91. Wang, S., Shao, J., Li, Z., Ren, Q., Yu, X.F., and Liu, S. (2019). Black phosphorus-based multimodal nanoagent: showing targeted combinatory therapeutics against cancer metastasis. Nano Lett. *19*, 5587–5594. https://doi.org/10.1021/acs.nanolett.9b02127.

92. Jin, Z., Duo, Y., Li, Y., Qiu, M., Jiang, M., Liu, Q., Zhao, P., Yang, T., Liang, W., Zhang, H., et al. (2021). A novel NIR-responsive CO gas-releasing and hyperthermia-generating nanomedicine provides a curative approach for cancer therapy. Nano Today *38*, 101197. https://doi.org/10.1016/j.nantod.2021.101197.

93. Zeng, C., Shang, W., Liang, X., Liang, X., Chen, Q., Chi, C., Du, Y., Fang, C., and Tian, J. (2016). Cancer diagnosis and imaging-guided photothermal therapy using a dual-modality nanoparticle. ACS Appl. Mater. Interfaces *8*, 29232–29241. https://doi.org/10.1021/acsami.6b06883.

94. Vankayala, R., and Hwang, K.C. (2018). Near-infrared-light-activatable nanomaterial-mediated phototheranostic nanomedicines: an emerging paradigm for cancer treatment. Adv. Mater. *30*, 1706320. https://doi.org/10.1002/adma.201706320.

95. Chen, W., Ouyang, J., Liu, H., Chen, M., Zeng, K., Sheng, J., Liu, Z., Han, Y., Wang, L., Li, J., et al. (2017). Black phosphorus nanosheet-based drug delivery system for synergistic photodynamic/photothermal/chemotherapy of cancer. Adv. Mater. *29*, 1603864. https://doi.org/10.1002/adma.201603864.

96. Zhang, C.J., Hu, Q., Feng, G., Zhang, R., Yuan, Y., Lu, X., and Liu, B. (2015). Image-guided combination chemotherapy and photodynamic therapy using a mitochondria-targeted molecular probe with aggregation-induced emission characteristics. Chem. Sci. *6*, 4580–4586. https://doi.org/10.1039/c5sc00826c.

97. Sun, L.D., Wang, Y.F., and Yan, C.H. (2014). Paradigms and challenges for bioapplication of rare earth upconversion luminescent nanoparticles: small size and tunable emission/excitation spectra. Acc. Chem. Res. *47*, 1001–1009. https://doi.org/10.1021/ar400218t.

98. Lv, R., Yang, D., Yang, P., Xu, J., He, F., Gai, S., Li, C., Dai, Y., Yang, G., and Lin, J. (2016). Integration of upconversion nanoparticles and ultrathin black phosphorus for efficient photodynamic theranostics under 808 nm near-infrared light irradiation. Chem. Mater. *28*, 4724–4734. https://doi.org/10.1021/acs.chemmater.6b01720.

99. Shen, J., Chen, G., Vu, A.M., Fan, W., Bilsel, O.S., Chang, C.C., and Han, G. (2013). Engineering the upconversion nanoparticle excitation wavelength: cascade sensitization of tri-doped upconversion colloidal nanoparticles at 800 nm. Adv. Opt. Mater. *1*, 644–650. https://doi.org/10.1002/adom.201300160.

100. Yang, G., Zhang, R., Liang, C., Zhao, H., Yi, X., Shen, S., Yang, K., Cheng, L., and Liu, Z. (2018). Manganese dioxide coated WS_2@Fe_3O_4/sSiO_2 nanocomposites for pH-responsive MR imaging and oxygen-elevated synergetic therapy. Small *14*, 1702664. https://doi.org/10.1002/smll.201702664.

101. Ge, X., Su, L., Yang, L., Fu, Q., Li, Q., Zhang, X., Liao, N., Yang, H., and Song, J. (2021). NIR-II fluorescent biodegradable nanoprobes for precise acute kidney/liver injury imaging and therapy. Anal. Chem. *93*, 13893–13903. https://doi.org/10.1021/acs.analchem.1c02742.

102. Cheng, G., Li, Z., Liu, Y., Ma, R., Chen, X., Liu, W., Song, Y., Zhang, Y., Yu, G., Wu, Z., and Chen, T. (2023). "Swiss Army Knife" black phosphorus-based nanodelivery platform for synergistic antiparkinsonian therapy via remodeling the brain microenvironment. J. Control. Release *353*, 752–766. https://doi.org/10.1016/j.jconrel.2022.12.024.

103. Lu, H., Wei, J., Liu, K., Li, Z., Xu, T., Yang, D., Gao, Q., Xiang, H., Li, G., and Chen, Y. (2023). Radical-scavenging and subchondral bone-regenerating nanomedicine for osteoarthritis treatment. ACS Nano *17*, 6131–6146. https://doi.org/10.1021/acsnano.3c01789.

104. Li, Z., Cai, F., Tang, J., Xu, Y., Guo, K., Xu, Z., Feng, Y., Xi, K., Gu, Y., and Chen, L. (2023). Oxygen metabolism-balanced engineered hydrogel microspheres promote the regeneration of the nucleus pulposus by inhibiting acid-sensitive complexes. Bioact. Mater. *24*, 346–360. https://doi.org/10.1016/j.bioactmat.2022.12.025.

105. He, Z., Chen, W., Hu, K., Luo, Y., Zeng, W., He, X., Li, T., Ouyang, J., Li, Y., Xie, L., et al. (2024). Resolvin D1 delivery to lesional macrophages using antioxidative black phosphorus nanosheets for atherosclerosis treatment. Nat. Nanotechnol. *19*, 1386–1398. https://doi.org/10.1038/s41565-024-01687-1.

106. Wang, L., Chen, F., Zhang, C., Cheng, Y.Y., Bu, W., and Liu, Y. (2024). Reactive oxygen species and neurodegenerative diseases: insights into nanozyme therapeutics. MedMat *1*, 55–73. https://doi.org/10.1097/mm9.0000000000000009.

107. Pedersen, J.T., Chen, S.W., Borg, C.B., Ness, S., Bahl, J.M., Heegaard, N.H.H., Dobson, C.M., Hemmingsen, L., Cremades, N., and Teilum, K. (2016). Amyloid-beta and alpha-synuclein decrease the level of metal-catalyzed reactive oxygen species by radical scavenging and redox silencing. J. Am. Chem. Soc. *138*, 3966–3969. https://doi.org/10.1021/jacs.5b13577.

108. Chen, W., Ouyang, J., Yi, X., Xu, Y., Niu, C., Zhang, W., Wang, L., Sheng, J., Deng, L., Liu, Y.N., and Guo, S. (2018). Black phosphorus nanosheets as a neuroprotective nanomedicine for neurodegenerative disorder therapy. Adv. Mater. *30*, 1703458. https://doi.org/10.1002/adma.201703458.

109. Kim, S.J., Han, H.H., and Hahn, S.K. (2021). Hyaluronate/black phosphorus complexes as a copper chelating agent for wilson disease treatment. Biomater. Res. *25*, 20–29. https://doi.org/10.1186/s40824-021-00221-x.

110. Ala, A., Walker, A.P., Ashkan, K., Dooley, J.S., and Schilsky, M.L. (2007). Wilson's disease. Lancet *369*, 397–408. https://doi.org/10.1016/S0140-6736(07)60196-2.

111. Tang, Z., Kong, N., Ouyang, J., Feng, C., Kim, N.Y., Ji, X., Wang, C., Farokhzad, O.C., Zhang, H., and Tao, W. (2020). Phosphorus science-oriented design and synthesis of multifunctional nanomaterials for biomedical applications. Matter *2*, 297–322. https://doi.org/10.1016/j.matt.2019.12.007.

112. He, M., Li, K., Yang, J., Wang, Q., and Gu, J. (2022). Photodynamic and its concomitant ion-interference synergistic therapies based on functional hierarchically mesoporous MOFs. Small *18*, 2204295. https://doi.org/10.1002/smll.202204295.

113. Zhou, W., Pan, T., Cui, H., Zhao, Z., Chu, P.K., and Yu, X.F. (2019). Black phosphorus: bioactive nanomaterials with inherent and selective chemotherapeutic effects. Angew. Chem. Int. Ed. *58*, 769–774. https://doi.org/10.1002/anie.201810878.

114. Kong, N., Ji, X., Wang, J., Sun, X., Chen, G., Fan, T., Liang, W., Zhang, H., Xie, A., Farokhzad, O.C., and Tao, W. (2020). ROS-mediated selective killing effect of black phosphorus: mechanistic understanding and its guidance for safe biomedical applications. Nano Lett. *20*, 3943–3955. https://doi.org/10.1021/acs.nanolett.0c01098.

115. Cheng, L., Chen, Z., Cai, Z., Zhao, J., Lu, M., Liang, J., Wang, F., Qi, J., Cui, W., and Deng, L. (2020). Bioinspired functional black phosphorus electrospun fibers achieving recruitment and biomineralization for staged bone regeneration. Small *16*, 2005433. https://doi.org/10.1002/smll.202005433.

116. Wang, Y., Hu, X., Zhang, L., Zhu, C., Wang, J., Li, Y., Wang, Y., Wang, C., Zhang, Y., and Yuan, Q. (2019). Bioinspired extracellular vesicles embedded with black phosphorus for molecular recognition-guided biomineralization. Nat. Commun. *10*, 2829. https://doi.org/10.1038/s41467-019-10761-5.

117. Pan, T., Fu, W., Xin, H., Geng, S., Li, Z., Cui, H., Zhang, Y., Chu, P.K., Zhou, W., and Yu, X.F. (2020). Calcium phosphate mineralized black phosphorous with enhanced functionality and anticancer bioactivity. Adv. Funct. Mater. *30*, 2003069. https://doi.org/10.1002/adfm.202003069.

118. Yang, B., Ding, L., Chen, Y., and Shi, J. (2020). Augmenting tumor-starvation therapy by cancer cell autophagy inhibition. Adv. Sci. *7*, 1902847. https://doi.org/10.1002/advs.201902847.

119. Jeon, S., Lee, J.H., Jang, H.J., Lee, Y.B., Kim, B., Kang, M.S., Shin, Y.C., Shin, D.M., Hong, S.W., and Han, D.W. (2021). Spontaneously promoted osteogenic differentiation of MC3T3-E1 preosteoblasts on ultrathin layers of black phosphorus. Mat. Sci. Eng. C-Mater. *128*, 112309. https://doi.org/10.1016/j.msec.2021.112309.

120. Wang, Z., Zhao, J., Tang, W., Hu, L., Chen, X., Su, Y., Zou, C., Wang, J., Lu, W.W., Zhen, W., et al. (2019). Multifunctional nanoengineered hydrogels consisting of black phosphorus nanosheets upregulate bone formation. Small *15*, 1901560. https://doi.org/10.1002/smll.201901560.

121. Tong, L., Liao, Q., Zhao, Y., Huang, H., Gao, A., Zhang, W., Gao, X., Wei, W., Guan, M., Chu, P.K., and Wang, H. (2019). Near-infrared light control of bone regeneration with biodegradable photothermal osteoimplant. Biomaterials *193*, 1–11. https://doi.org/10.1016/j.biomaterials.2018.12.008.

122. Anderson, H.C. (2003). Matrix vesicles and calcification. Curr. Rheumatol. Rep. *5*, 222–226. https://doi.org/10.1007/s11926-003-0071-z.

123. Shao, J., Ruan, C., Xie, H., Chu, P.K., and Yu, X.F. (2020). Photochemical activity of black phosphorus for near-infrared light controlled in situ biomineralization. Adv. Sci. *7*, 2000439. https://doi.org/10.1002/advs.202000439.

124. Jing, X., Xu, C., Su, W., Ding, Q., Ye, B., Su, Y., Yu, K., Zeng, L., Yang, X., Qu, Y., et al. (2023). Photosensitive and conductive hydrogel induced

innerved bone regeneration for infected bone defect repair. Adv. Healthc. Mater. *12*, 2201349. https://doi.org/10.1002/adhm.202201349.

125. Xu, Y., Xu, C., He, L., Zhou, J., Chen, T., Ouyang, L., Guo, X., Qu, Y., Luo, Z., and Duan, D. (2022). Stratified-structural hydrogel incorporated with magnesium-ion-modified black phosphorus nanosheets for promoting neuro-vascularized bone regeneration. Bioact. Mater. *16*, 271–284. https://doi.org/10.1016/j.bioactmat.2022.02.024.

126. Li, Z., Zhang, X., Ouyang, J., Chu, D., Han, F., Shi, L., Liu, R., Guo, Z., Gu, G.X., Tao, W., et al. (2021). Ca^{2+}-supplying black phosphorus-based scaffolds fabricated with microfluidic technology for osteogenesis. Bioact. Mater. *6*, 4053–4064. https://doi.org/10.1016/j.bioactmat.2021.04.014.

127. Wang, X., Yu, Y., Yang, C., Shao, C., Shi, K., Shang, L., Ye, F., and Zhao, Y. (2021). Microfluidic 3D printing responsive scaffolds with biomimetic enrichment channels for bone regeneration. Adv. Funct. Mater. *31*, 2105190. https://doi.org/10.1002/adfm.202105190.

128. Zhang, X., Li, Q., Li, L., Ouyang, J., Wang, T., Chen, J., Hu, X., Ao, Y., Qin, D., Zhang, L., et al. (2023). Bioinspired mild photothermal effect-reinforced multifunctional fiber scaffolds promote bone regeneration. ACS Nano *17*, 6466–6479. https://doi.org/10.1021/acsnano.2c11486.

129. He, M., Zhang, X., Ran, X., Zhang, Y., Nie, X., Xiao, B., Lei, L., Zhai, S., Zhu, J., Zhang, J., et al. (2024). Black phosphorus nanosheets protect neurons by degrading aggregative α-syn and clearing ROS in parkinson's disease. Adv. Mater. *36*, 2404576. https://doi.org/10.1002/adma.202404576.

130. Conner, S.D., and Schmid, S.L. (2003). Regulated portals of entry into the cell. Nature *422*, 37–44. https://doi.org/10.1038/nature01451.

131. Shao, X., Ding, Z., Zhou, W., Li, Y., Li, Z., Cui, H., Lin, X., Cao, G., Cheng, B., Sun, H., et al. (2021). Intrinsic bioactivity of black phosphorus nanomaterials on mitotic centrosome destabilization through suppression of PLK1 kinase. Nat. Nanotechnol. *16*, 1150–1160. https://doi.org/10.1038/s41565-021-00952-x.

132. Xiong, Y., He, C., Qi, J., Xiong, M., Liu, S., Zhao, J., Li, Y., Liu, G., and Deng, W. (2025). Black phosphorus nanosheets activate tumor immunity of glioblastoma by modulating the expression of the immunosuppressive molecule PD-L1. Biomaterials *317*, 123062. https://doi.org/10.1016/j.biomaterials.2024.123062.

133. He, L., Zhao, J., Li, H., Xie, B., Xu, L., Huang, G., Liu, T., Gu, Z., and Chen, T. (2023). Metabolic reprogramming of NK cells by black phosphorus quantum dots potentiates cancer immunotherapy. Adv. Sci. *10*, 2202519. https://doi.org/10.1002/advs.202202519.

134. Chen, L., Fan, Y., Jiang, N., Huang, X., Yu, M., Zhang, H., Xu, Z., He, D., Wang, Y., Ding, C., et al. (2025). An energy metabolism-engaged nanomedicine maintains mitochondrial homeostasis to alleviate cellular ageing. Nat. Nanotechnol. *20*, 1332–1344. https://doi.org/10.1038/s41565-025-01972-7.

135. Ma, M., Zhang, Y., Pu, K., and Tang, W. (2025). Nanomaterial-enabled metabolic reprogramming strategies for boosting antitumor immunity. Chem. Soc. Rev. *54*, 653–714. https://doi.org/10.1039/d4cs00679h.

136. Ou, W., Byeon, J.H., Thapa, R.K., Ku, S.K., Yong, C.S., and Kim, J.O. (2018). Plug-and-play nanorization of coarse black phosphorus for targeted chemo-photoimmunotherapy of colorectal cancer. ACS Nano *12*, 10061–10074. https://doi.org/10.1021/acsnano.8b04658.

137. Liang, X., Ye, X., Wang, C., Xing, C., Miao, Q., Xie, Z., Chen, X., Zhang, X., Zhang, H., and Mei, L. (2019). Photothermal cancer immunotherapy by erythrocyte membrane-coated black phosphorus formulation. J. Control. Release *296*, 150–161. https://doi.org/10.1016/j.jconrel.2019.01.027.

138. Qiu, M., Tulufu, N., Tang, G., Ye, W., Qi, J., Deng, L., and Li, C. (2024). Black phosphorus accelerates bone regeneration based on immunoregulation. Adv. Sci. *11*, 2304824. https://doi.org/10.1002/advs.202304824.

139. Li, Z., Hu, Y., Fu, Q., Liu, Y., Wang, J., Song, J., and Yang, H. (2020). NIR/ROS-responsive black phosphorus QD vesicles as immunoadjuvant carrier for specific cancer photodynamic immunotherapy. Adv. Funct. Mater. *30*, 1905758. https://doi.org/10.1002/adfm.201905758.

140. Zhang, Y., Cui, Z., Kong, H., Xia, K., Pan, L., Li, J., Sun, Y., Shi, J., Wang, L., Zhu, Y., and Fan, C. (2016). One-Shot immunomodulatory nanodiamond agents for cancer immunotherapy. Adv. Mater. *28*, 2699–2708. https://doi.org/10.1002/adma.201506232.

141. Li, Z., Fu, Q., Ye, J., Ge, X., Wang, J., Song, J., and Yang, H. (2020). Ag^{+}-coupled black phosphorus vesicles with emerging NIR-II photoacoustic imaging performance for cancer immune-dynamic therapy and fast wound healing. Angew. Chem. Int. Ed. *59*, 22202–22209. https://doi.org/10.1002/anie.202009609.

142. Xie, Z., Peng, M., Lu, R., Meng, X., Liang, W., Li, Z., Qiu, M., Zhang, B., Nie, G., Xie, N., et al. (2020). Black phosphorus-based photothermal therapy with aCD47-mediated immune checkpoint blockade for enhanced cancer immunotherapy. Light Sci. Appl. *9*, 161. https://doi.org/10.1038/s41377-020-00388-3.

143. Huang, X., Zhong, Y., Li, Y., Zhou, X., Yang, L., Zhao, B., Zhou, J., Qiao, H., Huang, D., Qian, H., and Chen, W. (2022). Black phosphorus-synergic nitric oxide nanogasholder spatiotemporally regulates tumor microenvironments for self-amplifying immunotherapy. ACS Appl. Mater. Interfaces *14*, 37466–37477. https://doi.org/10.1021/acsami.2c10098.

144. Wang, J., Yu, W., Shen, H., Sang, Y., Zhang, H., Zheng, B., Peng, X., Hu, Y., Ma, X., Yang, Z., and Yu, F. (2025). Therapeutic black phosphorus nanosheets elicit neutrophil response for enhanced tumor suppression. Adv. Sci. *12*, 2414779. https://doi.org/10.1002/advs.202414779.

145. Li, W.H., Wu, J.J., Wu, L., Zhang, B.D., Hu, H.G., Zhao, L., Li, Z.B., Yu, X.F., and Li, Y.M. (2021). Black phosphorous nanosheet: a novel immune-potentiating nanoadjuvant for near-infrared-improved immunotherapy. Biomaterials *273*, 120788. https://doi.org/10.1016/j.biomaterials.2021.120788.